Spring 5-31-1993

Adaptive two-stage detection scheme in synchronous two-user CDMA systems

Yong Jiang
New Jersey Institute of Technology

Copyright Warning & Restrictions

The copyright law of the United States (Title 17, United States Code) governs the making of photocopies or other reproductions of copyrighted material.

Under certain conditions specified in the law, libraries and archives are authorized to furnish a photocopy or other reproduction. One of these specified conditions is that the photocopy or reproduction is not to be "used for any purpose other than private study, scholarship, or research." If a, user makes a request for, or later uses, a photocopy or reproduction for purposes in excess of "fair use" that user may be liable for copyright infringement,

This institution reserves the right to refuse to accept a copying order if, in its judgment, fulfillment of the order would involve violation of copyright law.

Please Note: The author retains the copyright while the New Jersey Institute of Technology reserves the right to distribute this thesis or dissertation

Printing note: If you do not wish to print this page, then select "Pages from: first page # to: last page #" on the print dialog screen

ABSTRACT

Adaptive Two-Stage Detection Scheme in Synchronous Two-User CDMA Systems

by

Yong Jiang

A conventional single user detector is not optimum in the multiuser environment because the multiuser interference can not be modeled as an additive Gaussian process. Such a receiver is very vulnerable to the near-far situation. The receiver that is optimum for multiuser environment has high complexity and requires a knowledge of the received signal energies. Various versions of the receiver that handle the near-far situation have been proposed in the literature. In this work, an adaptive two-stage scheme for a synchronous two-user environment with unknown received energies is proposed. It consists of a tandem of the conventional receiver and the interference canceler whose weights are adjusted by an adaptive algorithm. The error probability was evaluated analytically and it was shown that the receiver provides performance that is satisfactory in the near-far scenarios.

ADAPTIVE TWO-STAGE DETECTION SCHEME IN SYNCHRONOUS TWO-USER CDMA SYSTEMS

by

Yong Jiang

A Thesis
Submitted to the Faculty of
New Jersey Institute of Technology
in Partial Fulfillment of the Requirements for the Degree of
Master of Science in Electrical Engineering

Department of Electrical and Computer Engineering

May 1993

APPROVAL PAGE

Adaptive Two-Stage Detection Scheme in Synchronous Two-User CDMA Systems

Yong Jiang

Dr. Zoran Siveski, Thesis Advisor (date)
Assistant Professor of Electrical Engineering
New Jersey Institute of Technology

Dr. Yeheskel Bar-Ness, Committee Member (date)
Director of the Center for Communications and Signal Processing Research
Distinguished Professor of Electrical Engineering
New Jersey Institute of Technology

Dr. Alexander Haimovich, Committee Member (date)
Associate Professor of Electrical Engineering
New Jersey Institute of Technology

BIOGRAPHICAL SKETCH

Author: Yong Jiang

Degree: Master of Science in Electrical Engineering

Date: May 1993

Undergraduate and Graduate Education:

- Master of Science in Electrical Engineering,
  New Jersey Institute of Technology, Newark, NJ, 1993
- Bachelor of Science in Electrical Engineering,
  Shanghai Jiao Tong University, Shanghai, P. R. China, 1989

Major: Electrical Engineering

This thesis is dedicated to

my parents and my sister

ACKNOWLEDGMENT

I wish to acknowledge Professor Zoran Siveski, my advisor, for steering me toward projects which have helped me gain a better understanding of the field of communication. I have profited greatly from his guidance and insight.

Thanks are also due to other members of my thesis committee, Dr. Yeheskel Bar-Ness and Dr. Alexander Haimovich for their many constructive comments and suggestions concerning this work.

I am also grateful to my fellow researchers and friends in the Center for Communications and Signal Processing Research and the Department of Electrical and Computer Engineering at New Jersey Institute of Technology. Their input has helped me in all aspects of developing the research presented in this thesis. Special thanks to Mr. Zeeman Zhang for assisting me in editing.

Finally, I would like to extend special thanks to my parents and my sister for their eternal love and support during my years in graduate study.

TABLE OF CONTENTS

LIST OF FIGURES

Figure **Page**

Figure **Page**

CHAPTER 1

INTRODUCTION

In wireless personal and mobile communication the main issue in demodulation of digital signals sent simultaneously by several transmitters who share a multiple access channel is the selection of the multiplexing format. Compared to the well known multiple access techniques like frequency division multiple access (FDMA, all users transmit simultaneously in different frequency bands) and time division multiple access (TDMA, all users occupy the same bandwidth but transmit in different time slots), code division multiple access (CDMA) allows all the users to transmit at the same time and to occupy the entire available bandwidth. In CDMA, each user is assigned a distinct signature sequence which is used to modulate his message. To demodulate, the conventional single-user detector is implemented, which correlates the received signal with each of the signature sequences as if other users did not exist in the common channel. Besides the desired signal, the sampled output of each correlator contains the residual interference from all other users. Under the condition that the received signal energies are similar, the amount of interference can be reduced by choosing the signature sequences so that their crosscorrelations are low enough. However, if strong interferences are presented, i.e. some users are very week in comparison to others, it is unable to recover the message of the weak users reliably, even if the signature sequences have very low crosscorrelations. This is referred to as the near-far problem. To solve the problem, the traditional ways are the design of signals with more stringent crosscorrelation properties and power control, which is the adaptive adjustment of transmitter power depending on its location and on the received powers of the other users. This comes at the price in the multiple access capability reduction and bandwidth and complexity increase.

The fact that the residual interference at the output of each correlator can not be modeled as an additive white Gaussian process makes the conventional detector not optimal. By assuming the knowledge of each user's energy and the signature sequence, optimum detection can be achieved that maximizes the log-likelihood function. The structure of the optimum multiuser detector consists of a matched filter front-end followed by the decision system. The algorithm that decision system implements is the Viterbi algorithm [1]. For two users, the optimum solution is one of the four possible values of the vector of data bits. However, with the increase of the number of user, the complexity goes up exponentially. Therefore, lower complexity multiuser detectors are desired whose performance is close to the one of the optimum detector.

Several suboptimum multiuser detectors have been proposed, one of which is presented in [3], where the tentative decisions obtained with the conventional single-user detector depending on the polarity of the outputs of the matched filters, are weighted and subtracted from the output of the matched filter. The weights are fixed since the energies of the signals are known.

Instead from the conventional single-user detector, the tentative decisions can be obtained from a decorrelator, which removes the interference without knowing the energies of input signals. The error probability of one user at the output of the decorrelator is invariant with regard to the strength of the signals of other users, while its signal-to-noise ratio is less than in the single user case. In [3], the outputs of the decorrelator, considered as bit estimates, are weighted and utilized to cancel the interference from the outputs of matched filters. Again, the weights are fixed with the knowledge of input signals' energies.

The need of the knowledge of the information of received energies results in the increased price for it requires to estimate the energy of each user. One should consider other approaches that do not require the knowledge of the energy of each user. An adaptive algorithm well known as "Bootstrap Algorithm" introduced in [2],

offers the possibility of implementation in the CDMA systems. The weights in the second stage are to be adjusted adaptively so that the interference can be removed by subtracting the weighed bit estimates from the outputs of matched filters without the knowledge of the received energy. In this work, a synchronous two-user detector is discussed, where adaptive canceler is applied in the second stage, and the energies of input signals are assumed unknown. The output error probability is computed and simulated to compare to those for the conventional receiver, decorrelating detector and the detector in [3]. The convergence speed of the adaptive iteration is also observed.

CHAPTER 2

DETECTION IN SYNCHRONOUS CDMA SYSTEMS

2.1 Conventional Single-user Detector

A two-user synchronous CDMA receiver is shown as in Figure 2.1, which is referred to as a conventional single-user detector. The filter is matched to the signature sequence of each user. The data bit estimates are the hard limiter's outputs of the matched filters.

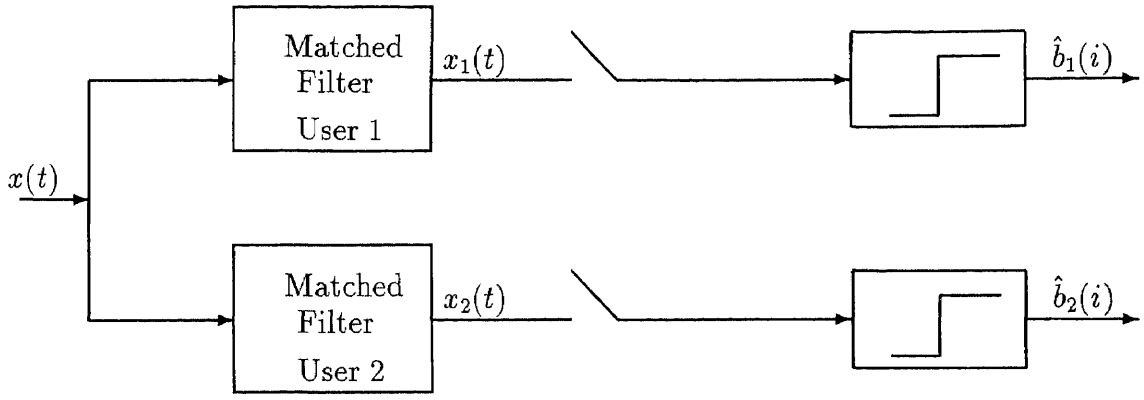

Figure 2.1 A synchronous two-user conventional CDMA receiver

The input signal can be written as

$$x(t) = \sum_{i=-M}^{M} b_1(i)\sqrt{A_1}s_1(t-iT) + \sum_{i=-M}^{M} b_2(i)\sqrt{A_2}s_2(t-iT) + n(t) \qquad (2.1)$$

where n(t) is white Gaussian noise with zero mean and power spectral density of $N_0/2$. The symbol streams $\{b_1(i)\}$ and $\{b_2(i)\}$ take values on $\{-1, 1\}$, A_1 and A_2 are their energies respectively. The unit-energy signature sequences assigned to both users are $s_1(t)$ and $s_2(t)$ and have duration T. The outputs of the matched filters are expressed as

$$x_1(i) = \sqrt{A_1}b_1(i) + \rho\sqrt{A_2}b_2(i) + n_1(i)$$

$$x_2(i) = \sqrt{A_2}b_2(i) + \rho\sqrt{A_1}b_1(i) + n_2(i) \tag{2.2}$$

with

$$\int_0^T s_j^2(t)dt = 1, \text{for j=1, 2} \tag{2.3}$$

and

$$\rho = \int_0^T s_1(t)s_2(t)dt \tag{2.4}$$

$n_1(i)$ and $n_2(i)$ are zero mean Gaussian random variables having variance $N_0/2$ and crosscorrelation $\rho N_0/2$. After decision, the outputs are

$$\hat{b}_1(t) = sgn[x_1(i)]$$

$$\hat{b}_2(t) = sgn[x_2(i)] \tag{2.5}$$

For the sake of brevity, time index i is omitted from most of the expressions in the text.

In (2.2), besides the desired signals, the interferences caused by the other user also exists. The performance of the conventional single-user detector is acceptable provided the similarity of the energies of the received signals and/or the low cross-correlations of the signature waveforms. In practice, unfortunately, one user is often much stronger than the other so that the weaker user becomes undetectable, even if the signature waveforms have very low crosscorrelations. This problem, known as "near-far" problem is the main shortcoming of the conventional single-user detector.

2.2 Optimum Detector

Figure 2.2 gives an optimum detector. The optimum or the maximum likelihood decision on $b_1(i)$ and $b_2(i)$ denoted by $\hat{b}_1(i)$ and $\hat{b}_2(i)$ is one that maximizes the log-likelihood function. Noticing that in (2.1) the noise is white and Gaussian, assuming

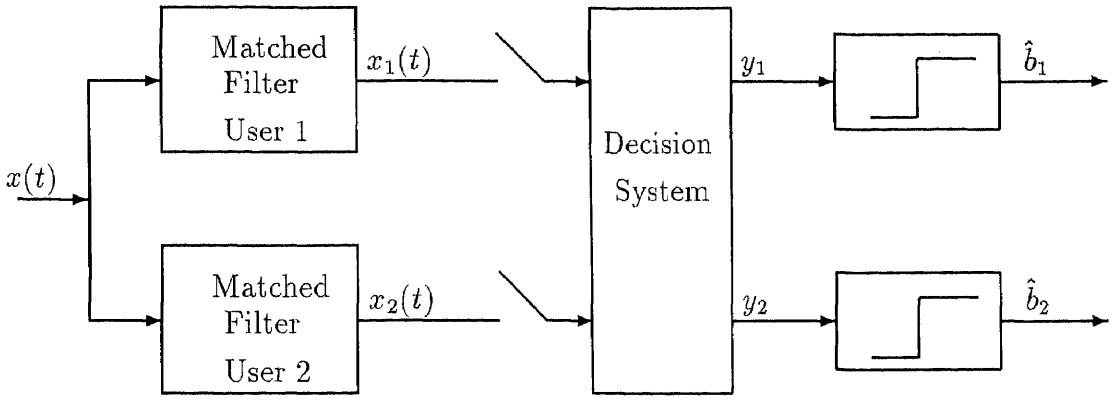

Figure 2.2 Optimum two-user detector

that the optimum detector knows the received energies, it should select the argument to achieve

$$min\left\{\int_0^T\left[x(t)-\sum_{k=1}^{2}\sqrt{A_k}\hat{b}_k(0)s_k(0)\right]^2 dt\right\} = max\left\{2(\mathbf{A}\hat{\mathbf{b}})^T\mathbf{x}-(\mathbf{A}\hat{\mathbf{b}})^T\mathbf{H}(\mathbf{A}\hat{\mathbf{b}})\right\} \tag{2.6}$$

where

$$\mathbf{x} = [x_1(0), x_2(0)]^T$$

$$\hat{\mathbf{b}} = [\hat{b_1}(0), \hat{b_2}(0)]$$

and

$$\mathbf{H} = \begin{bmatrix} 1 & \rho \\ \rho & 1 \end{bmatrix}$$

$$\mathbf{A} = \begin{bmatrix} \sqrt{A_1} & 0 \\ 0 & \sqrt{A_2} \end{bmatrix}$$

It is easy to solve the right-hand side of (2.6). Since $\hat{b}_k(0) \in \{-1, 1\}$, the function therein can be computed for each of the four possible values of $\hat{\mathbf{b}}$ and the vector that maximizes the function gives the solution to the optimum demodulation problem. In the K-user case, there are 2^K possible values of $\hat{\mathbf{b}}$ meaning that the complexity increases exponentially with the number of users.

The optimum detector provides important performance improvement over the conventional single-user detector, and in particular, it solves the near-far problem.

However, the price for this is exponential complexity in the number of users. Low complexity multiuser detectors are desired whose performance will be close to the performance of the optimum detector.

2.3 Suboptimum Detector

Due to the high complexity of the optimum detector, one should consider a suboptimum detector with satisfactory performance and simpler algorithm. Instead of the optimum decision system in Figure 2.2, an interference canceler is employed, as shown in Figure 2.3.

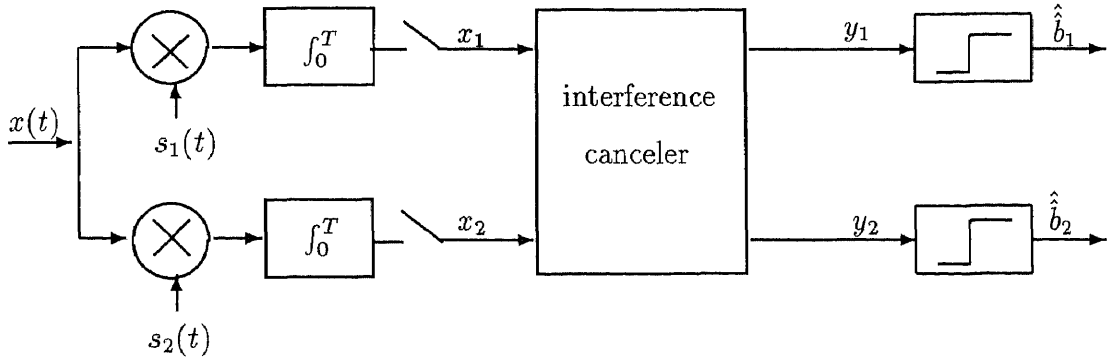

Figure 2.3 Suboptimum two-user detector

Various schemes of interference canceling have been proposed, two of them are discussed bellow.

2.3.1 Bit Estimates Obtained with the Conventional Single-user Detector

An approach to obtain suboptimum multiuser signal detector [1] is shown in Figure 2.4 where the estimates, $\hat{b_1}$ and $\hat{b_2}$ are obtained from the conventional detector.

$$\hat{b_1} = sgn(x_1) \tag{2.7}$$

$$\hat{b_2} = sgn(x_2) \tag{2.8}$$

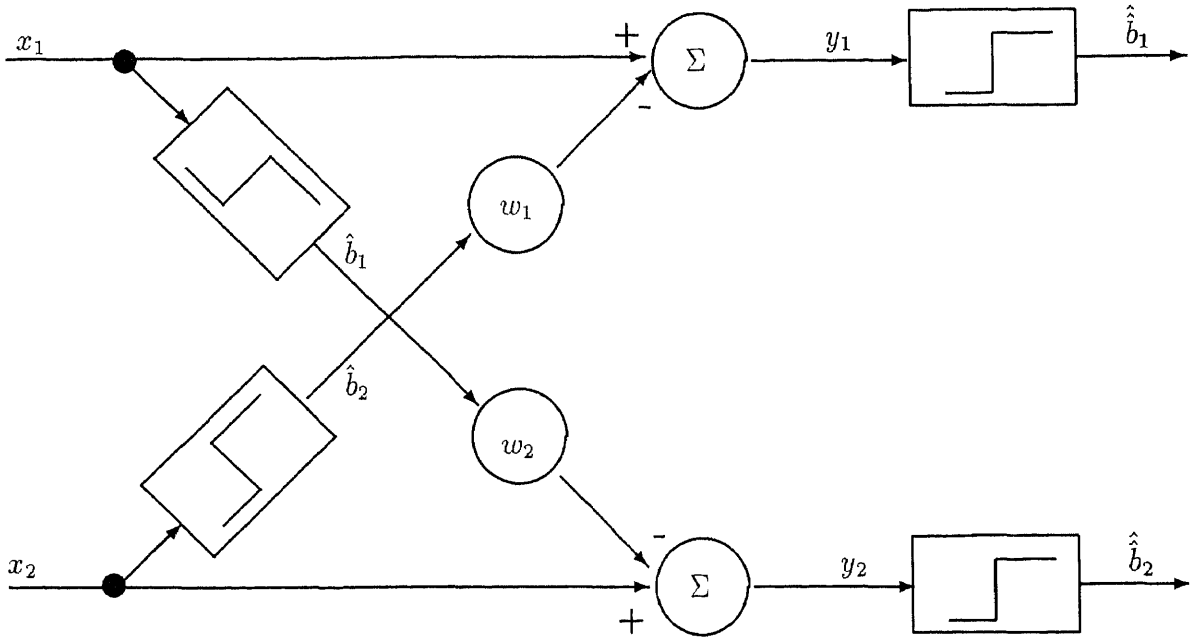

Figure 2.4 Two-stage receiver for two synchronous users, with bit estimates obtained by conventional detector.

Since the received energies are assumed known, the weights are set as

$$w_1 = \rho\sqrt{A_2}$$

and

$$w_2 = \rho\sqrt{A_1}$$

yielding the outputs of the second stage, before the decision:

$$\begin{aligned} y_1 &= \sqrt{A_1}b_1 + \rho\sqrt{A_2}b_2 - w_1\hat{b}_2 + n_1 \\ &= \sqrt{A_1}b_1 + \rho\sqrt{A_2}(b_2 - \hat{b}_2) + n_1 \end{aligned} \tag{2.9}$$

$$\begin{aligned} y_2 &= \sqrt{A_2}b_2 + \rho\sqrt{A_1}b_1 - w_2\hat{b}_1 + n_2 \\ &= \sqrt{A_2}b_2 + \rho\sqrt{A_1}(b_1 - \hat{b}_1) + n_2 \end{aligned} \tag{2.10}$$

If the signal of user 2 is comparatively strong, the conventional detector will select $\hat{b}_2 = b_2$ with high probability, in which case the interference caused by user 2 will be canceled effectively, and therefore, the decision on the bit transmitted by user 1 can be noticeably improved. On the other hand, the decision on the bit of user 2 will not get improved since $\hat{b}_1 = b_1$ does not occur with high enough probability.

2.3.2 Bit Estimates Obtained by Decorrelator

In [3] Varanasi and Aazhang proposed another approach to obtain suboptimum multiuser signal detector, shown as Figure 2.5.

The reference estimates are the outputs of a decorrelator instead of the conventional detector which was used in Section 2.3.1. The outputs of the decorrelator are

$$\begin{aligned} z_1 &= x_1 - \rho x_2 \\ &= (1-\rho^2)\sqrt{A_1}b_1 + n_1 - \rho n_2 \end{aligned} \tag{2.11}$$

$$\begin{aligned} z_2 &= x_2 - \rho x_1 \\ &= (1-\rho^2)\sqrt{A_2}b_2 + n_2 - \rho n_1 \end{aligned} \tag{2.12}$$

The corresponding bit estimates are

$$\begin{aligned} \hat{b_1} &= sgn(z_1) \\ &= sgn[(1-\rho^2)\sqrt{A_1}b_1 + n_1 - \rho n_2] \end{aligned} \tag{2.13}$$

$$\begin{aligned} \hat{b_2} &= sgn(z_2) \\ &= sgn[(1-\rho^2)\sqrt{A_2}b_2 + n_2 - \rho n_1] \end{aligned} \tag{2.14}$$

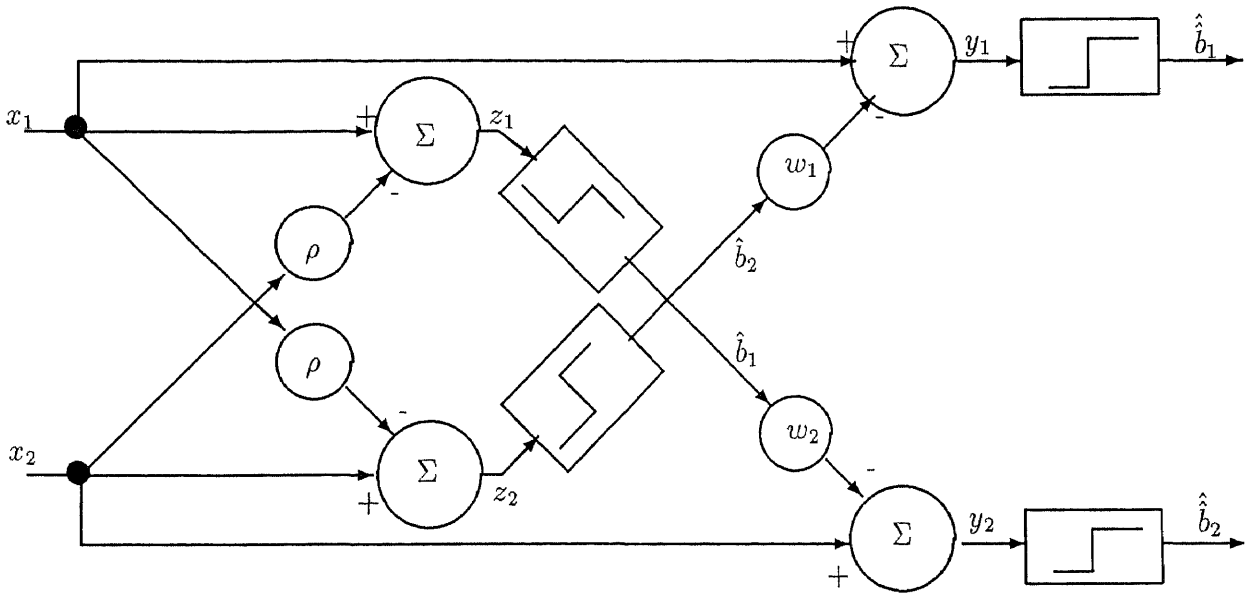

Figure 2.5 Two-stage receiver for two synchronous users with bit estimates obtaine d by decorrelator.

Define

$$\eta_1 = n_1 - \rho n_2 \tag{2.15}$$

and

$$\eta_2 = n_2 - \rho n_1 \tag{2.16}$$

It is easy to show

$$E\{\eta_1\} = E\{\eta_2\} = 0$$

$$\begin{aligned} E\{\eta_1^2\} &= E\{n_1^2 + \rho^2 n_2^2 - 2\rho n_1 n_2\} \\ &= \frac{N_0}{2} + \rho^2 \frac{N_0}{2} - 2\rho^2 \frac{N_0}{2} \\ &= (1-\rho^2)\frac{N_0}{2} \end{aligned} \tag{2.17}$$

and

$$E\{\eta_2^2\} = (1-\rho^2)\frac{N_0}{2} \tag{2.18}$$

$$\begin{aligned} E\{\eta_1 n_2\} &= E\{n_1 n_2\} - \rho E\{n_2^2\} \\ &= \rho\sigma^2 - \rho\sigma^2 \\ &= 0 \end{aligned} \tag{2.19}$$

similarly

$$E\{\eta_2 n_1\} = 0 \tag{2.20}$$

also

$$\begin{aligned} E\{n_1\hat{b_2}\} &= E\left\{n_1 sgn[(1-\rho^2)\sqrt{A_2}b_2 + \eta_2]\right\} \\ &= 0 \end{aligned} \tag{2.21}$$

$$\begin{aligned} E\{b_1\hat{b_2}\} &= E\left\{b_1 sgn[(1-\rho^2)\sqrt{A_2}b_2 + \eta_2]\right\} \\ &= 0 \end{aligned} \tag{2.22}$$

Similarly

$$E\{n_2\hat{b_1}\} = 0 \tag{2.23}$$

$$E\{b_2\hat{b_1}\} = 0 \tag{2.24}$$

With the knowledge of the received signals' energies, the weights are fixed as

$$w_1 = \rho\sqrt{A_2}$$

and

$$w_2 = \rho\sqrt{A_1}$$

Therefore, the outputs of the canceler, before the decision, are

$$\begin{aligned} y_1 &= \sqrt{A_1}b_1 + \rho\sqrt{A_2}b_2 - w_1\hat{b_2} + n_1 \\ &= \sqrt{A_1}b_1 + \rho\sqrt{A_2}(b_2 - \hat{b_2}) + n_1 \end{aligned} \tag{2.25}$$

and

$$\begin{aligned} y_2 &= \sqrt{A_2}b_2 + \rho\sqrt{A_1}b_1 - w_2\hat{b_1} + n_2 \\ &= \sqrt{A_2}b_2 + \rho\sqrt{A_1}(b_1 - \hat{b_1}) + n_2 \end{aligned} \tag{2.26}$$

The error performance of bit estimates $\hat{b_1}$ and $\hat{b_2}$ in (2.13) and (2.14), which are the outputs of decorrelating detector, remains invariant to interference signal strengths. In fact, the error performance depends on the signal-to-noise ratio at the outputs of the decorrelating detector. Consider z_1, the SNR of z_1 is

$$\begin{aligned} SNR_{z_1} &= \frac{(1-\rho^2)^2 A_1}{(1-\rho^2)N_0} \\ &= (1-\rho^2)\frac{A_1}{N_0} \\ &= (1-\rho^2)SNR_1 \end{aligned} \tag{2.27}$$

where $SNR_1 = A_1/N_0$ is the received signal-to-noise ratio of user 1. SNR_{z_1} is reduced by $(1-\rho^2)$ after decorrelating. If SNR_1 is large enough, $\hat{b_1}$ can be detected as b_1 at a high probability, hence the bit transmitted by user 1 is correctly recovered. Same results can be obtained for user 2.

CHAPTER 3

ADAPTIVE SEPARATION OF SUPERIMPOSED SIGNALS

In code division multiple access (CDMA) systems, the received signal can be considered as a superimposed signal in which desired signal needs to be separated from the interference. An approach is proposed in [2] referred to as "a bootstrapped algorithm", in which each of the outputs of the separator is used as a reference input to an least mean square (LMS) algorithm which produce the other output. For simplicity, all signals discussed here are assumed real.

3.1 The Forward-Forward Structure

Consider a two-user case as in Figure 3.1, the model is

$$\mathbf{x}(t) = \mathbf{A}\mathbf{s}(t) + \mathbf{n}(t) \tag{3.1}$$

where

$$\mathbf{x}(t) = [s_1(t)s_2(t)]^T$$

$$\mathbf{n}(t) = [n_1(t)n_2(t)]^T$$

$$\mathbf{A} = \begin{bmatrix} 1 & a_1 \\ a_2 & 1 \end{bmatrix}$$

The assumption that $a_{11} = a_{22} = 1$ does not set any limitation since the power of the signals is assumed unknown. Separation is performed to use a 2×2 matrix $\mathbf{w}_{ff}$ to make

$$\mathbf{y}(t) = \mathbf{w}_{ff}\mathbf{x}(t) = \hat{\mathbf{s}}(t) \tag{3.2}$$

where $\hat{\mathbf{s}}(t)$ is the estimate of $\mathbf{s}(t)$.

In Figure 3.1 a cross-coupled forward-forward structure is depicted. w_1 and w_2 are weights. The relation between input and output can be written as

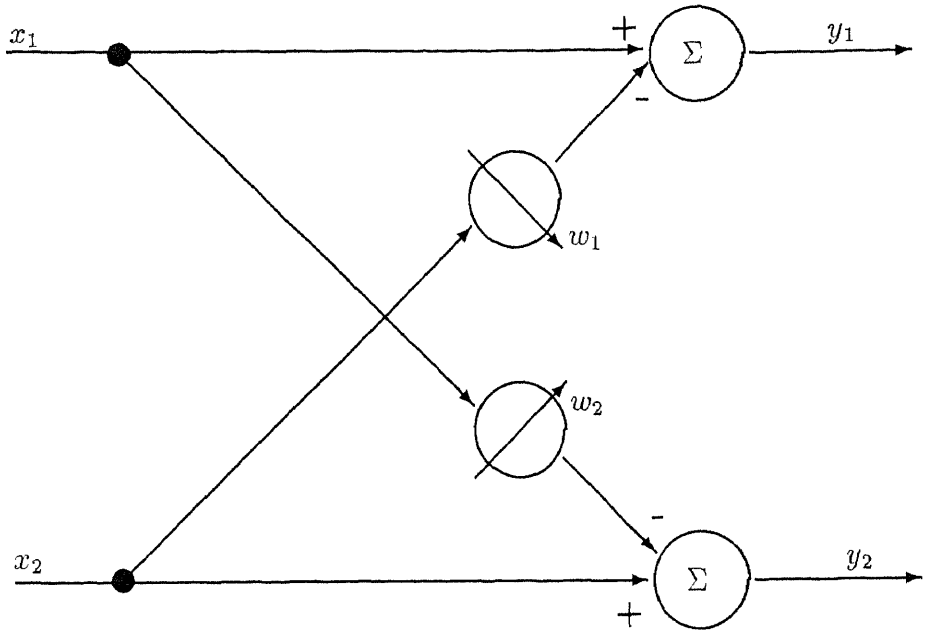

Figure 3.1 A forward-forward adaptive separator

$$\mathbf{y}(t) = \mathbf{w}_{ff}\mathbf{x}(t) \tag{3.3}$$

where

$$\mathbf{w}_{ff} = \begin{bmatrix} 1 & -w_1 \\ -w_2 & 1 \end{bmatrix} \tag{3.4}$$

Substituting (3.1) into (3.2) we get

$$\begin{aligned} \mathbf{y} &= \mathbf{w}_{ff}\mathbf{A}\mathbf{s} + \mathbf{w}_{ff}\mathbf{n} \\ &= \mathbf{H}_{ff}\mathbf{s} + \mathbf{n}_{ff} \end{aligned} \tag{3.5}$$

where

$$\mathbf{H}_{ff} = \begin{bmatrix} 1 - w_1 a_2 & a_1 - w_1 \\ a_2 - w_2 & 1 - w_2 a_1 \end{bmatrix} \tag{3.6}$$

and

$$\mathbf{n}_{ff} = \mathbf{w}_{ff}\mathbf{n} \tag{3.7}$$

To separate the signals, w_1 and w_2 are supposed to be chosen so that $\mathbf{H}_{ff}$ is a diagonal matrix. Therefore, the desired solution is

$$w_1 = a_1 \tag{3.8}$$

$$w_2 = a_2 \tag{3.9}$$

for which

$$\mathbf{H}_{ff} = \begin{bmatrix} 1 - a_1 a_2 & 0 \\ 0 & 1 - a_1 a_2 \end{bmatrix} \tag{3.10}$$

The output correlation matrix is given by

$$\begin{aligned} \mathbf{R}_{ff} &= E\left[\mathbf{y}(t)\mathbf{y}^T(t)\right] \\ &= \mathbf{H}_{ff}\mathbf{R}_s\mathbf{H}_{ff}^T + \mathbf{w}_{ff}\mathbf{R}_n\mathbf{w}_{ff}^T \end{aligned} \tag{3.11}$$

where

$$\mathbf{R}_s = E\left\{\mathbf{s}(t)\mathbf{s}^T(t)\right\}$$

and

$$\mathbf{R}_n = E\left\{\mathbf{n}(t)\mathbf{n}^T(t)\right\}$$

The signal vectors are assumed uncorrelated, then

$$\mathbf{R}_s = \begin{bmatrix} \sigma_1^2 & 0 \\ 0 & \sigma_2^2 \end{bmatrix} \tag{3.12}$$

$$\mathbf{R}_n = \begin{bmatrix} N_0/2 & 0 \\ 0 & N_0/2 \end{bmatrix} \tag{3.13}$$

where σ_1^2 and σ_2^2 are the power of $s_1(t)$ and $s_2(t)$ respectively, $N_0/2$ is the variance of $n_1(t)$ and $n_2(t)$ which are uncorrelated process. By substituting (3.10), (3.12) and (3.13) into (3.11) we get

$$\mathbf{R}_{ff} = \begin{bmatrix} r_{11} & r_{12} \\ r_{21} & r_{22} \end{bmatrix} + \frac{N_0}{2}\begin{bmatrix} 1 + w_1^2 & -(w_1 + w_2) \\ -(w_1 + w_2) & 1 + w_2^2 \end{bmatrix} \tag{3.14}$$

where

$$r_{11} = \sigma_1^2(1 - w_1 a_2)^2 + \sigma_2^2(a_1 - w_1)^2$$

$$r_{12} = \sigma_1^2(a_2 - w_2)(1 - w_1 a_2) + \sigma_2^2(a_1 - w_1)(1 - w_2 a_1) = r_{21}$$

$$r_{22} = \sigma_1^2(a_2 - w_2)^2 + \sigma_2^2(1 - w_2 a_1)^2 \tag{3.15}$$

It is stated in [2] that, for $N_0/2 = 0$ (no noise), $\mathbf{H}_{ff}$ is diagonal if and only if $\mathbf{R}_{ff}$ is. Therefore, decorrelation of the output signal is a useful criterion for signal separation, i.e.

$$E\{y_1(t)y_2(t)\} = 0 \tag{3.16}$$

In Figure 3.1, the upper loop attempts to cancel the interference caused by $s_2(t)$, while the lower loop attempts to cancel interference caused by $s_1(t)$. The bootstrapping results from control on both weights w_1 and w_2. It was shown that the resultant algorithm converges to the unique solution $w_1 = a_1$ and $w_2 = a_2$ if noise power is zero ($N_0/2 = 0$) and $|a_1| < 1$, $|a_2| < 1$. At the same time, the output signals are given by

$$y_1(t) = (1 - a_1 a_2)s_1(t) \tag{3.17}$$

$$y_2(t) = (1 - a_1 a_2)s_2(t) \tag{3.18}$$

That is, the signals are indeed separated but are scaled by a factor which is related to the model parameters.

3.2 The Backward-Backward Structure

In Figure 3.2, a backward-backward structure is depicted. The output-input relation is given by

$$\mathbf{y}(t) = \mathbf{w}_{bb}\mathbf{x}(t) = \hat{\mathbf{s}}(t) \tag{3.19}$$

where

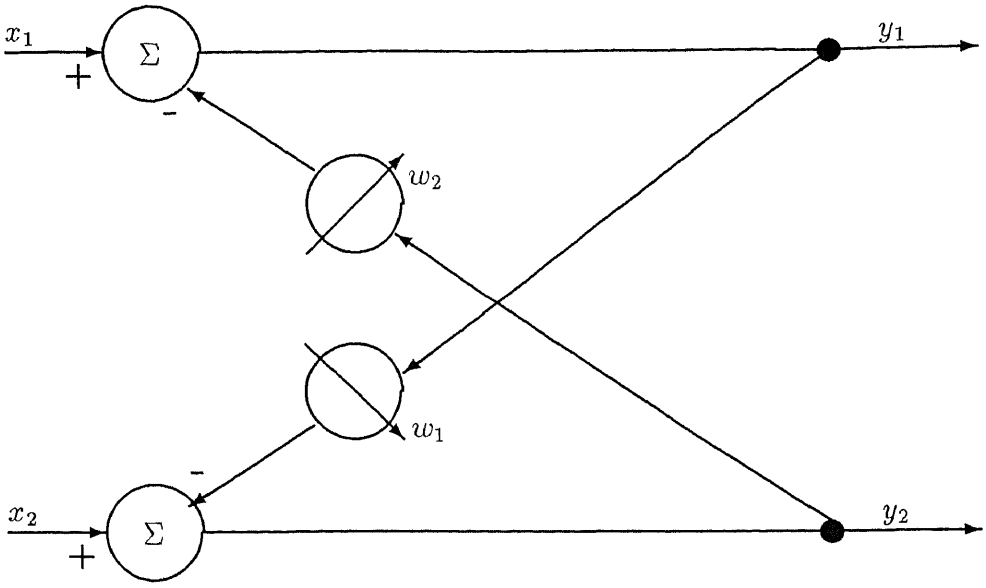

Figure 3.2 A backward-backward adaptive separator

$$\begin{aligned} \mathbf{w}_{bb} &= \frac{1}{1-w_1w_2}\begin{bmatrix} 1 & -w_1 \\ -w_2 & 1 \end{bmatrix} \\ &= \frac{1}{1-w_1w_2}\mathbf{w}_{ff} \end{aligned} \tag{3.20}$$

in which $\mathbf{w}_{ff}$ is given in (3.4). Since $\mathbf{w}_{bb}$ and $\mathbf{w}_{ff}$ differ only by the scalar factor $1/(1-w_1w_2)$, we can easily adopt the results of Section 3.1 to this case. In particular

$$\mathbf{y} = \mathbf{H}_{bb}\mathbf{s} + \mathbf{w}_{bb}\mathbf{n} \tag{3.21}$$

where

$$\mathbf{H}_{bb} = \frac{1}{(1-w_1w_2)^2}\mathbf{H}_{ff}$$

The desired solution still is

$$\begin{aligned} w_1 &= a_1 \\ w_2 &= a_2 \end{aligned} \tag{3.22}$$

The output correlation matrix is given by

$$\begin{aligned} \mathbf{R}_{bb} &= E\{\mathbf{y}(t)\mathbf{y}^T(t)\} \\ &= \frac{1}{(1-w_1w_2)^2}\mathbf{R}_{ff} \end{aligned} \tag{3.23}$$

where $\mathbf{R}_{ff}$ is given in (3.14). In [2] it is indicated that, when $N_0/2 = 0$ (no noise), the two output powers are minimized if and only if (3.22) is satisfied. Thus, simultaneous minimization of both output powers has been proposed as an optimization criterion. Notice that, equating the derivative of the output power to zero is a necessary condition of minimization, that is

$$\begin{aligned} \frac{d}{dw_1}E\{y_1^2(t)\} &= E\left\{\frac{d}{dw_1}[x_1(t)-w_1y_2(t)]^2\right\} \\ &= -2E\{y_1(t)y_2(t)\} \\ &= 0 \end{aligned} \tag{3.24}$$

and similarly

$$\frac{d}{dw_2}E\{y_2^2(t)\} = -2E\{y_1(t)y_2(t)\} = 0 \tag{3.25}$$

From (3.24) and (3.25) we can conclude that the minimum crosscorrelation between two outputs is the necessary condition for minimum output powers. Therefore, in this configuration, decorrelation of outputs and minimization of their powers are equivalent. however, this conclusion does not hold for forward-forward structure, in which case the assignment of the above mentioned derivative to zero gives

$$\begin{aligned} \frac{d}{dw_1}E\{y_1^2(t)\} &= E\left\{\frac{d}{dw_1}[x_1(t)-w_1x_2(t)]^2\right\} \\ &= -2E\{x_2(t)y_1(t)\} \\ &= 0 \end{aligned} \tag{3.26}$$

and similarly

$$\frac{d}{dw_2}E\{y_2^2(t)\} = -2E\{x_1(t)y_2(t)\} = 0 \tag{3.27}$$

which does not lead to the diagonal matrix of $\mathbf{R}_{ff}$.

CHAPTER 4

ADAPTIVE TWO-USER CDMA DETECTION

In Chapter 3 an approach of separation of superimposed signals was presented. It has been applied on the two-user CDMA detection in which the various control schemes on weight update control are employed. It is assumed that the received energies of the signals are unknown.

4.1 Adaptive Detection with Bit Estimates Obtained from the Outputs of the Matched Filters

4.1.1 Scheme

We consider a two-user synchronous CDMA receiver with the interference canceler of the forward-forward structure, as shown in Figure 4.1.

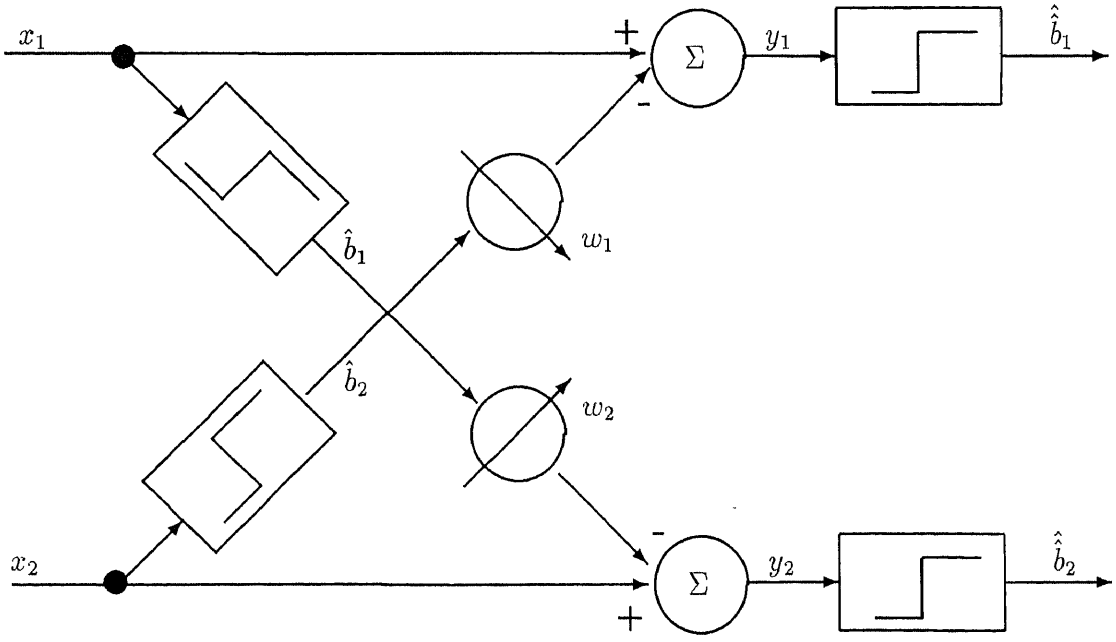

Figure 4.1 A two-user synchronous CDMA receiver with the bit estimates obtained by conventional detector.

It is similar to the one introduced in Section 2.3.1 with the difference that the weights are to be updated adaptively. As discussed in Section 3.1, it is indicated that decorrelation of the output signals can be a criterion for the signal separation in forward-forward structure, that is, using

$$E\{y_1(t)y_2(t)\} = 0$$

Here, the output powers $E\{y_1^2\}$ and $E\{y_2^2\}$ will be minimized simultaneously by the control algorithm of iterative search

$$w_j(n+1) = w_j(n) - \mu \frac{dE\{y_j^2(n)\}}{dw_j}, j = 1, 2 \tag{4.1}$$

where μ is the convergence and stability rate constant, n is the index of iteration. The optimum weights that minimize the output powers are the steady state values obtained from

$$\frac{dE\{y_1^2\}}{dw_1} = 0$$

and

$$\frac{dE\{y_2^2\}}{dw_2} = 0$$

Noticing that $y_1 = x_1 - w_1\hat{b}_2$ and $y_2 = x_2 - w_2\hat{b}_1$, we get

$$\begin{aligned} \frac{d}{dw_1} E\left\{(x_1 - w_1\hat{b}_2)^2\right\} &= E\left\{(x_1 - w_1\hat{b}_2)(-\hat{b}_2)\right\} \\ &= 0 \end{aligned} \tag{4.2}$$

and

$$\begin{aligned} \frac{d}{dw_2} E\left\{(x_2 - w_2\hat{b}_1)^2\right\} &= E\left\{(x_2 - w_2\hat{b}_1)(-\hat{b}_1)\right\} \\ &= 0 \end{aligned} \tag{4.3}$$

From (4.2) we get

$$-E\left\{x_1\hat{b}_2\right\} + w_1 \underbrace{E\left\{\hat{b}_2\hat{b}_2\right\}}_{1} = 0$$

that is

$$\begin{aligned} w_{10} &= E\{x_1\hat{b}_2\} \\ &= \sqrt{A_1}E\{b_1\hat{b}_2\} + \rho\sqrt{A_2}E\{b_2\hat{b}_2\} + E\{n_1\hat{b}_2\} \end{aligned} \tag{4.4}$$

Similarly

$$w_{20} = \sqrt{A_2}E\{b_2\hat{b}_1\} + \rho\sqrt{A_1}E\{b_1\hat{b}_1\} + E\{n_2\hat{b}_1\} \tag{4.5}$$

The right-hand side of (4.3) is the crosscorrelation of the output of one user and the bit estimate of the other user.

$$E\left\{(x_2 - w_2\hat{b}_1)(-\hat{b}_1)\right\} = E\{-y_2\hat{b}_1\}$$

Therefore (4.1) can be written as

$$w_j(n+1) = w_j(n) + \mu E\{y_2(n)\hat{b}_1(n)\}$$

The convergence speed is controled by scalar μ.

The outputs of the canceler are

$$y_1 = \sqrt{A_1}b_1 + \rho\sqrt{A_2}b_2 - w_1\hat{b}_2 + n_1 \tag{4.6}$$

$$y_2 = \sqrt{A_2}b_2 + \rho\sqrt{A_1}b_1 - w_2\hat{b}_1 + n_2 \tag{4.7}$$

After substituting (4.4),(4.5) into (4.6) and (4.7), the canceler outputs become

$$y_{10} = \sqrt{A_1}[b_1 - E\{b_1\hat{b}_2\}\hat{b}_2] + \rho\sqrt{A_2}[b_2 - E\{b_2\hat{b}_2\}\hat{b}_2] + E\{n_1\hat{b}_2\} + n_1 \tag{4.8}$$

$$y_{20} = \sqrt{A_2}[b_2 - E\{b_2\hat{b}_1\}\hat{b}_1] + \rho\sqrt{A_1}[b_1 - E\{b_1\hat{b}_1\}\hat{b}_1] + E\{n_2\hat{b}_1\} + n_2 \tag{4.9}$$

The joint statistics appearing in above expressions will be evaluated in terms of the system's parameters in Section 4.1.2.

If the bit estimates of the sampled correlator's outputs are almost perfect, i.e. $\hat{b}_1 \simeq b_1$ and $\hat{b}_2 \simeq b_2$, then

$$E\{b_1\hat{b}_2\} \simeq 0$$

$$E\{b_2\hat{b}_2\} \simeq 1$$

and

$$E\{b_2\hat{b}_1\} \simeq 0$$

$$E\{b_1\hat{b}_1\} \simeq 1$$

This will make the canceler output, from (4.8) and (4.9), become interference free, i.e.

$$y_1 \simeq \sqrt{A_1}b_1 + n_1$$

and

$$y_2 \simeq \sqrt{A_2}b_2 + n_2$$

The respective signal-to-noise ratios $SNR_1 = A_1/N_0$ and $SNR_2 = A_2/N_0$ will determine the error performance. To get clean bit estimates $\hat{b}_1$ and $\hat{b}_2$, it requires a low spectral efficiency (small ρ). In the mean time, both large and approximately equal SNRs are also required to achieve the above results. If the power of one of the signals is much larger than that of the other, say $\rho^2 SNR_2 \gg SNR_1$, i.e. $\rho\sqrt{A_2} \gg \sqrt{A_1}$, $\hat{b}_2$ will still be an almost perfect estimate of b_2, on which case $w_{10} \simeq \rho\sqrt{A_2}$ from (4.4). At the same time, however, $x_1 = \sqrt{A_1}b_1 + \rho\sqrt{A_2}b_2 + n_2$ is dominated by b_2, which is the interference caused by user 2. This will lead to $\hat{b}_1 \simeq b_2$, hence, from (4.5), $w_{20} \simeq \sqrt{A_2}$ and from (4.9), $y_{20} \simeq \rho\sqrt{A_1}b_1 + n_2$, in which the desired signal b_2 is cancelled. A disastrous output performance of b_2 occurs because of the power inversion effect of the canceler.

To solve the problem, the control algorithm has to be rectified. One way of doing so is to add a constraint to the iterative algorithm so that at any bit interval, the weights are set such that

$$w_j = min\{w_1, w_2\}, j = 1, 2 \tag{4.10}$$

The restriction effectively prevents the increase of the weight that affects the stronger signal which can achieve perfect decision without the canceler. Under such constraint, w_{20} will be replaced by smaller one, $w_{10} \simeq \rho\sqrt{A_2}$, resulting in the second output

$$y_2 \simeq (1-\rho)\sqrt{A_2}b_2 + \rho\sqrt{A_1}b_1 + n_2$$

This will definitely better than the output without constraint. The amount of improvement depends on the desired component to the residual interference ratio at the output, which is $[(1-\rho)/\rho]^2 \Delta SNR$.

Since it is unnecessary to perform canceling on the much stronger signal, another constraint can be considering as "disabling" the canceling loop that contains the larger weight element, that is

$$max\{w_1, w_2\} = 0 \tag{4.11}$$

In the case discussed above, it means $w_2 = 0$. Therefore the decision output of the larger signal comes directly from the input signal. This scheme can be successful to obtain perfect detection when $\rho^2 SNR_2 \gg SNR_1$.

4.1.2 Error Performance

The bit estimates at the output are defined as

$$\hat{\hat{b}}_1 = sgn(y_1)$$

$$\hat{\hat{b}}_2 = sgn(y_2) \tag{4.12}$$

The two-user error probabilities $Po_1(\epsilon)$ and $Po_2(\epsilon)$ are conditional error probabilities averaged over b_1, b_2, $\hat{b}_2$ and b_1, b_2, $\hat{b}_1$, respectively.

Consider the detector in Figure 4.1. Without loss of generality, consider user 1 first:

$$
\begin{aligned}
Po_1(\epsilon) &= E_{b_1,b_2,\hat{b_2}} Pr\{\hat{\hat{b}}_1 \text{ in error} | b_1, b_2, \hat{b}_2\} \\
&= \frac{1}{2} \sum_{b_2,\hat{b_2}} [Pr(n_1 > \sqrt{A_1} - \rho\sqrt{A_2} b_2 + w_{10}\hat{b}_2) \\
&\qquad + Pr(n_1 < -\sqrt{A_1} - \rho\sqrt{A_2} b_2 + w_{10}\hat{b}_2)] \\
&= \frac{1}{2} \sum_{b_2} \Big[Pr(n_1 > \sqrt{A_1} - \rho\sqrt{A_2} b_2 - w_{10}, \hat{b}_2 = -1) \\
&\qquad + Pr(n_1 < -\sqrt{A_1} - \rho\sqrt{A_2} b_2 - w_{10},\ hat b_2 = -1) \\
&\qquad + Pr(n_1 > \sqrt{A_1} - \rho\sqrt{A_2} b_2 + w_{10}, \hat{b}_2 = 1) \\
&\qquad + Pr(n_1 < -\sqrt{A_1} - \rho\sqrt{A_2} b_2 + w_{10}, \hat{b}_2 = 1) \Big] \\
&= \frac{1}{2} \sum_{b_2} \Big[Pr(n_1 > \sqrt{A_1} - \rho\sqrt{A_2} b_2 - w_{10}, n_2 < -\sqrt{A_2} b_2 + \rho\sqrt{A_1}) \\
&\qquad + Pr(n_1 < -\sqrt{A_1} - \rho\sqrt{A_2} b_2 - w_{10}, n_2 < -\sqrt{A_2} b_2 - \rho\sqrt{A_1}) \\
&\qquad + Pr(n_1 > \sqrt{A_1} - \rho\sqrt{A_2} b_2 + w_{10}, n_2 > -\sqrt{A_2} b_2 + \rho\sqrt{A_1}) \\
&\qquad + Pr(n_1 < -\sqrt{A_1} - \rho\sqrt{A_2} b_2 + w_{10}, n_2 > -\sqrt{A_2} b_2 - \rho\sqrt{A_1}) \Big] \\
&= \frac{1}{4} \Big[Pr(n_1 > \sqrt{A_1} + \rho\sqrt{A_2} - w_{10}, n_2 < \sqrt{A_2} + \rho\sqrt{A_1}) \\
&\qquad + Pr(n_1 < -\sqrt{A_1} + \rho\sqrt{A_2} - w_{10}, n_2 < \sqrt{A_2} - \rho\sqrt{A_1}) \\
&\qquad + Pr(n_1 > \sqrt{A_1} + \rho\sqrt{A_2} + w_{10}, n_2 > \sqrt{A_2} + \rho\sqrt{A_1}) \\
&\qquad + Pr(n_1 < -\sqrt{A_1} + \rho\sqrt{A_2} + w_{10}, n_2 > \sqrt{A_2} - \rho\sqrt{A_1}) \Big] \\
&\qquad + Pr(n_1 > \sqrt{A_1} - \rho\sqrt{A_2} - w_{10}, n_2 < -\sqrt{A_2} + \rho\sqrt{A_1}) \\
&\qquad + Pr(n_1 < -\sqrt{A_1} - \rho\sqrt{A_2} - w_{10}, n_2 < -\sqrt{A_2} - \rho\sqrt{A_1}) \\
&\qquad + Pr(n_1 > \sqrt{A_1} - \rho\sqrt{A_2} + w_{10}, n_2 > -\sqrt{A_2} + \rho\sqrt{A_1}) \\
&\qquad + Pr(n_1 < -\sqrt{A_1} - \rho\sqrt{A_2} + w_{10}, n_2 > -\sqrt{A_2} - \rho\sqrt{A_1}) \Big]
\end{aligned}
$$

$$
\begin{aligned}
&= \frac{1}{2}\Big[Pr(n_1 > \sqrt{A_1} + \rho\sqrt{A_2} - w_{10}, n_2 < \sqrt{A_2} + \rho\sqrt{A_1}) \\
&\quad + Pr(n_1 > \sqrt{A_1} - \rho\sqrt{A_2} - w_{10}, n_2 < -\sqrt{A_2} + \rho\sqrt{A_1}) \\
&\quad + Pr(n_1 > \sqrt{A_1} + \rho\sqrt{A_2} + w_{10}, n_2 > \sqrt{A_2} + \rho\sqrt{A_1}) \\
&\quad + Pr(n_1 > \sqrt{A_1} - \rho\sqrt{A_2} + w_{10}, n_2 > -\sqrt{A_2} + \rho\sqrt{A_1})\Big] \\
&= \frac{1}{2}\sum_{i=1}^{4}\int\int_{D_i} f_{n_1,n_2}(n_1,n_2)dn_1dn_2 \qquad (4.13)
\end{aligned}
$$

where

$$
f_{n_1,n_2}(n_1,n_2) = \frac{1}{\pi N_0\sqrt{1-\rho^2}} exp\left[-\frac{n_1^2 - 2\rho n_1 n_2 + n_2^2}{N_0(1-\rho^2)}\right] \qquad (4.14)
$$

and the regions of integration are

$$
\begin{aligned}
D_1 &: \left\{n_1 > \sqrt{A_1} + \rho\sqrt{A_2} - w_{10}, n_2 < \sqrt{A_2} + \rho\sqrt{A_1}\right\} \\
D_2 &: \left\{n_1 > \sqrt{A_1} - \rho\sqrt{A_2} - w_{10}, n_2 < -\sqrt{A_2} + \rho\sqrt{A_1}\right\} \\
D_3 &: \left\{n_2 > \sqrt{A_2} + \rho\sqrt{A_1} + w_{10}, n_1 > \sqrt{A_1} + \rho\sqrt{A_2}\right\} \\
D_4 &: \left\{n_2 > \sqrt{A_2} - \rho\sqrt{A_1} + w_{10}, n_1 > -\sqrt{A_1} + \rho\sqrt{A_2}\right\}
\end{aligned}
$$

To evaluate the optimum weights, rewrite (4.4) and (4.5) as follows

$$
w_{10} = \sqrt{A_1}E\{b_1\hat{b}_2\} + \rho\sqrt{A_2}E\{b_2\hat{b}_2\} + E\{n_1\hat{b}_2\}
$$

$$
w_{20} = \sqrt{A_2}E\{b_2\hat{b}_1\} + \rho\sqrt{A_1}E\{b_1\hat{b}_1\} + E\{n_2\hat{b}_1\}
$$

The joint statistics are derived as follows:

$$
E\{b_1\hat{b_1}\} = Pr\{b_1 = \hat{b}_1\} - Pr\{b_1 \neq \hat{b}_1\} \qquad (4.15)
$$

Denote the error probability of the bit estimates $\hat{b_1}$ and $\hat{b_2}$ as $Pi_1(\epsilon)$ and $Pi_2(\epsilon)$ respectively, i.e.

$$
Pi_1(\epsilon) = Pr(b_1 \neq \hat{b_1})
$$

$$
Pi_2(\epsilon) = Pr(b_2 \neq \hat{b_2})
$$

then

$$\begin{aligned} E\{b_1\hat{b_1}\} &= [1 - P_{i1}(\epsilon)] - P_{i1}(\epsilon) \\ &= 1 - 2P_{i1}(\epsilon) \end{aligned}$$

However

$$\begin{aligned} P_{i1}(\epsilon) &= Pr\{\hat{b}_1 \text{ in error}\} \\ &= E_{b_1,b_2} Pr\{\hat{b_1} \text{ in error}|b_1, b_2\} \\ &= \frac{1}{4}\sum_{b_2}\left[Pr\{n_1 > \sqrt{A_1} - \rho\sqrt{A_2}b_2\} + Pr\{n_1 < -\sqrt{A_1} - \rho\sqrt{A_2}b_2\}\right] \end{aligned}$$

Average over both values of b_2,

$$P_{i1}(\epsilon) = \frac{1}{2}\left[Q\left(\frac{\sqrt{A_1} - \rho\sqrt{A_2}}{\sqrt{N_0/2}}\right) + Q\left(\frac{\sqrt{A_1} + \rho\sqrt{A_2}}{\sqrt{N_0/2}}\right)\right]$$

where

$$Q(x) = \frac{1}{\sqrt{2\pi}}\int_x^\infty e^{-t^2/2}dt$$

Similarly,

$$\begin{aligned} P_{i2}(\epsilon) &= Pr\{\hat{b}_2 \text{ in error}\} \\ &= \frac{1}{2}\left[Q\left(\frac{\sqrt{A_2} - \rho\sqrt{A_1}}{\sqrt{N_0/2}}\right) + Q\left(\frac{\sqrt{A_2} + \rho\sqrt{A_1}}{\sqrt{N_0/2}}\right)\right] \end{aligned}$$

Therefore

$$E\{b_1\hat{b_1}\} = 1 - Q\left(\frac{\sqrt{A_1} + \rho\sqrt{A_2}}{\sqrt{N_0/2}}\right) - Q\left(\frac{\sqrt{A_1} - \rho\sqrt{A_2}}{\sqrt{N_0/2}}\right) \tag{4.16}$$

Also

$$\begin{aligned} E\{b_2\hat{b_2}\} &= 1 - 2P_{i1}(\epsilon) \\ &= 1 - Q\left(\frac{\sqrt{A_2} + \rho\sqrt{A_1}}{\sqrt{N_0/2}}\right) - Q\left(\frac{\sqrt{A_2} - \rho\sqrt{A_1}}{\sqrt{N_0/2}}\right) \end{aligned} \tag{4.17}$$

$$
\begin{aligned}
E\{b_1\hat{b_2}\} &= E_{b_1,b_2}\{b_1 sgn[\sqrt{A_2}b_2+\rho\sqrt{A_1}b_1+n_2]\} \\
&= \frac{1}{4}\sum_{b_1,b_2} b_1\left[Pr\{n_2 > -\sqrt{A_2}b_2-\rho\sqrt{A_1}b_1\} - Pr\{n_2 < -\sqrt{A_2}b_2-\rho\sqrt{A_1}b_1\}\right] \\
&= \frac{1}{4}\sum_{b_1,b_2} b_1\left[2Q\left(\frac{-\sqrt{A_2}b_2-\rho\sqrt{A_1}b_1}{\sqrt{N_0/2}}\right)-1\right] \\
&= \frac{1}{4}\sum_{b_2}\left[2Q\left(\frac{-\sqrt{A_2}b_2-\rho\sqrt{A_1}}{\sqrt{N_0/2}}\right)-1-2Q\left(\frac{-\sqrt{A_2}b_2+\rho\sqrt{A_1}}{\sqrt{N_0/2}}\right)+1\right] \\
&= \frac{1}{2}\left[Q\left(\frac{-\sqrt{A_2}-\rho\sqrt{A_1}}{\sqrt{N_0/2}}\right)+Q\left(\frac{\sqrt{A_2}-\rho\sqrt{A_1}}{\sqrt{N_0/2}}\right)\right. \\
&\quad \left. -Q\left(\frac{-\sqrt{A_2}+\rho\sqrt{A_1}}{\sqrt{N_0/2}}\right)-Q\left(\frac{\sqrt{A_2}+\rho\sqrt{A_1}}{\sqrt{N_0/2}}\right)\right] \\
&= \frac{1}{2}\left\{\left[1-2Q\left(\frac{\sqrt{A_2}+\rho\sqrt{A_1}}{\sqrt{N_0/2}}\right)\right]-\left[1-2Q\left(\frac{\sqrt{A_2}-\rho\sqrt{A_1}}{\sqrt{N_0/2}}\right)\right]\right\} \\
&= Q\left(\frac{\sqrt{A_2}-\rho\sqrt{A_1}}{\sqrt{N_0/2}}\right)-Q\left(\frac{\sqrt{A_2}+\rho\sqrt{A_1}}{\sqrt{N_0/2}}\right) \qquad (4.18)
\end{aligned}
$$

Similarly,

$$
E\{b_2\hat{b_1}\} = Q\left(\frac{\sqrt{A_1}-\rho\sqrt{A_2}}{\sqrt{N_0/2}}\right)-Q\left(\frac{\sqrt{A_1}+\rho\sqrt{A_2}}{\sqrt{N_0/2}}\right) \qquad (4.19)
$$

$$
\begin{aligned}
E\{n_1\hat{b_2}\} &= E\{n_1 sgn(\sqrt{A_2}b_2+\rho\sqrt{A_1}b_1+n_2)\} \\
&= \frac{1}{4}\sum_{b_1,b_2}\left[\int_{-\infty}^{\infty}\int_{-\sqrt{A_2}b_2-\rho\sqrt{A_1}b_1}^{\infty} n_1 f_{n_1,n_2}(n_1,n_2)dn_1dn_2\right. \\
&\qquad \left. -\int_{-\infty}^{\infty}\int_{-\infty}^{-\sqrt{A_2}b_2-\rho\sqrt{A_1}b_1} n_1 f_{n_1,n_2}(n_1,n_2)dn_1dn_2\right] \\
&= \frac{1}{4}\sum_{i=1}^{4}\left[\int\int_{D_i} n_1 f_{n_1,n_2}(n_1,n_2)dn_1dn_2\right. \\
&\qquad \left. -\int\int_{S_i} n_1 f_{n_1,n_2}(n_1,n_2)dn_1dn_2\right] \qquad (4.20)
\end{aligned}
$$

where the integral regions are

$$
\begin{aligned}
D_1 &: \{-\infty < n_1 < \infty, -\sqrt{A_2}-\rho\sqrt{A_1} < n_2 < \infty\} \\
D_2 &: \{-\infty < n_1 < \infty, -\sqrt{A_2}+\rho\sqrt{A_1} < n_2 < \infty\}
\end{aligned}
$$

$$
\begin{aligned}
D_3 &: \{-\infty < n_1 < \infty, \sqrt{A_2} - \rho\sqrt{A_1} < n_2 < \infty\} \\
D_4 &: \{-\infty < n_1 < \infty, \sqrt{A_2} + \rho\sqrt{A_1} < n_2 < \infty\} \\
S_1 &: \{-\infty < n_1 < \infty, -\infty < n_2 < -\sqrt{A_2} - \rho\sqrt{A_1}\} \\
S_2 &: \{-\infty < n_1 < \infty, -\infty < n_2 < -\sqrt{A_2} + \rho\sqrt{A_1}\} \\
S_3 &: \{-\infty < n_1 < \infty, -\infty < n_2 < \sqrt{A_2} - \rho\sqrt{A_1}\} \\
S_4 &: \{-\infty < n_1 < \infty, -\infty < n_2 < \sqrt{A_2} + \rho\sqrt{A_1}\}
\end{aligned}
$$

Similarly,

$$
\begin{aligned}
E\{n_2\hat{b_1}\} = \frac{1}{4}\sum_{i=1}^{4}\Big[\int\int_{D_i} n_2 f_{n_1,n_2}(n_1,n_2)dn_1dn_2 \\
- \int\int_{S_i} n_2 f_{n_1,n_2}(n_1,n_2)dn_1dn_2\Big] \qquad (4.21)
\end{aligned}
$$

where the integral regions are

$$
\begin{aligned}
D_1 &: \{-\sqrt{A_1} - \rho\sqrt{A_2} < n_1 < \infty, -\infty < n_2 < \infty\} \\
D_2 &: \{-\sqrt{A_1} + \rho\sqrt{A_2} < n_1 < \infty, -\infty < n_2 < \infty\} \\
D_3 &: \{\sqrt{A_1} - \rho\sqrt{A_2} < n_1 < \infty, -\infty < n_2 < \infty\} \\
D_4 &: \{\sqrt{A_1} + \rho\sqrt{A_2} < n_1 < \infty, -\infty < n_2 < \infty\} \\
S_1 &: \{-\infty < n_1 < -\sqrt{A_1} - \rho\sqrt{A_2}, -\infty < n_2 < \infty\} \\
S_2 &: \{-\infty < n_1 < -\sqrt{A_1} + \rho\sqrt{A_2}, -\infty < n_2 < \infty\} \\
S_3 &: \{-\infty < n_1 < \sqrt{A_1} - \rho\sqrt{A_2}, -\infty < n_2 < \infty\} \\
S_4 &: \{-\infty < n_1 < \sqrt{A_1} + \rho\sqrt{A_2}, -\infty < n_2 < \infty\}
\end{aligned}
$$

With the constraint scheme in either (4.10) or (4.11), the optimum weights w_{10} and w_{20} in the above expressions should be modified accordingly.

Numerical results are computed with respect to the signal-to-noise ratios and crosscorrelation coefficients. The curves are plotted versus the difference of the two input SNRs. As before, SNR_1 is kept constant. the error probabilities of conventional receiver and the decorrelating detector in [3] with fixed weights are also presented.

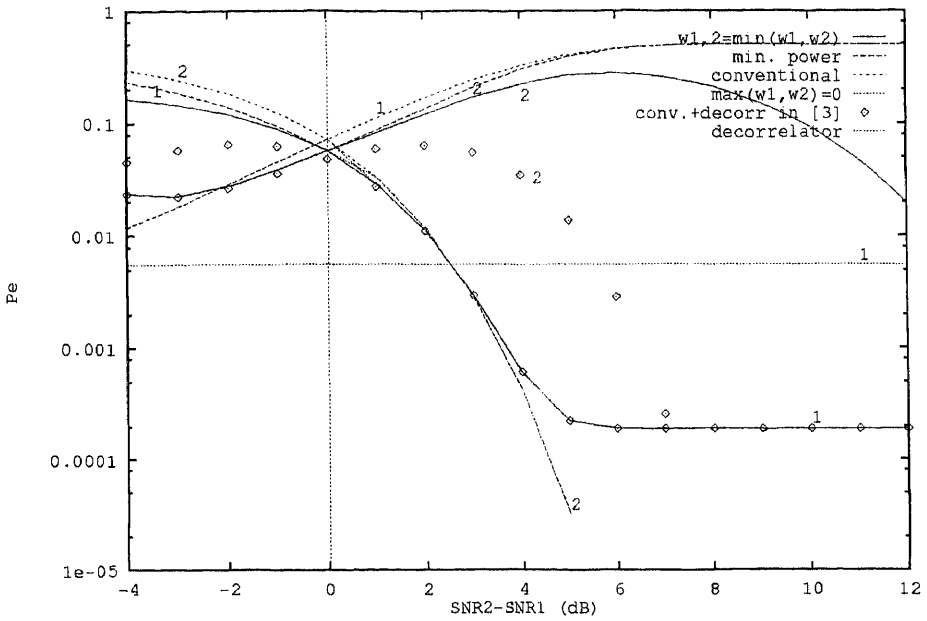

Figure 4.2 Computed error performance with bit estimates obtained from conventiona l detector with $\rho = 0.7$, and $SNR_1 = 8$ dB.

In Figure 4.2 $\rho = 0.7$ is used. the performance of user 1 in conventional detection is too poor to be detected as ΔSNR goes high, reaching an error probability of 0.5, which shows the vulnerability of the conventional detector to the near-far problem. As predicted, the curve of minimum power of user 2 also approaches to 0.5 when ΔSNR becomes larger, because of the reason that was discussed in Section 4.1.1. Marginal improvement occurs at large ΔSNR when constraint from (4.10) is imposed. More ever, with the constraint from (4.11), an excellent performance is achieved which is even better than that in [3]. The performance of user 1 keeps unchanged no matter whether the constraint strategies are used when $\Delta SNR > 0$ dB. This results from the fact that the constraint strategies are designed to prevent the stronger user (user 2 in this case) from being canceled due to the power inversion effect.

Figure 4.3 depicts the case for $\rho = 0.5$. A better performance of user 2 under constraints from (4.10) is observed than that of previous case. Again, as expected, the performance of user 1 is virtually the same as that in [3]. This results from the

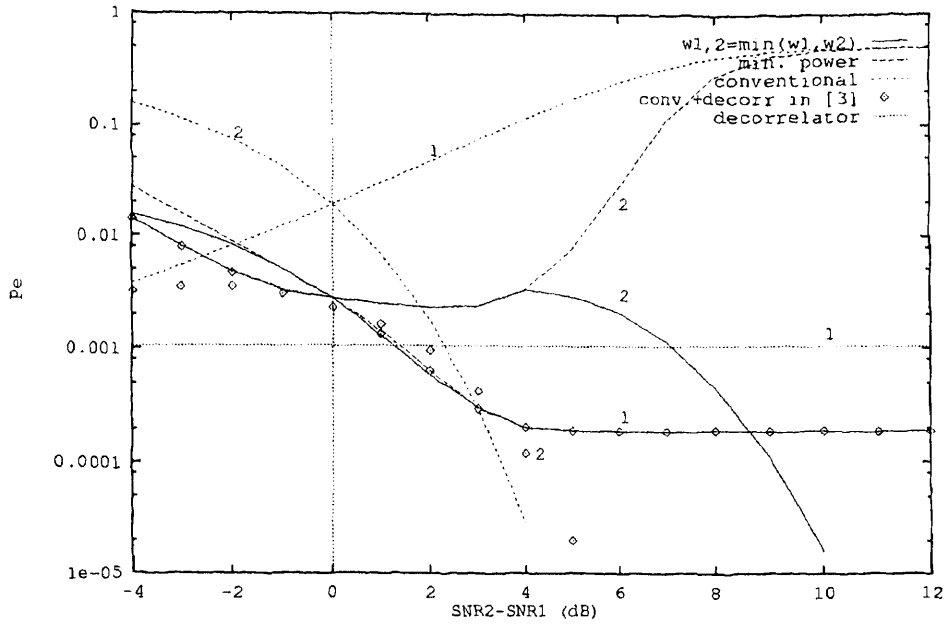

Figure 4.3 Computed error performance with bit estimates obtained from conventiona l detector with $\rho = 0.5$, and $SNR_1 = 8$ dB.

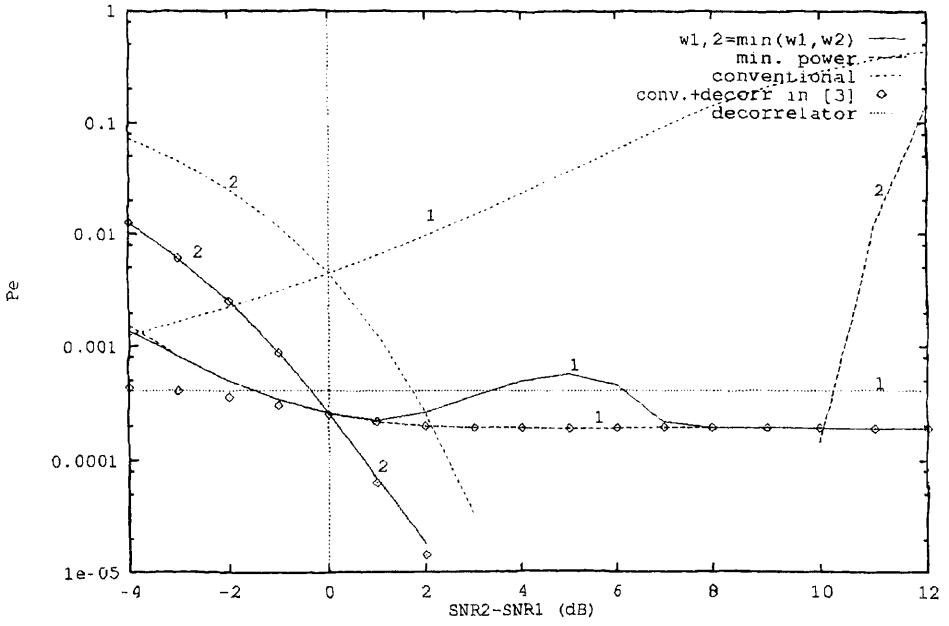

Figure 4.4 Computed error performance with bit estimates obtained from conventiona l detector with $\rho = 1/3$, and $SNR_1 = 8$ dB.

factor $[(1-\rho)/\rho]^2$ being greater in this case.

Figure 4.4 is the case for $\rho = 1/3$. the deterioration in the performance of user 2 for very high ΔSNR, as predicted, is due to the fact that $\rho^2 SNR_2 \gg SNR_1$mentioned in Section 4.1.1. With the constraint from (4.10) the curve of user 2 matches that of [3], while the performance of user 1 is slightly degraded over a limited range of ΔSNRs.

4.1.3 Simulation

1. Simulation on error performance

Numerical results from simulation of the error probability are presented as functions of signal-to-noise ratio and the crosscorrelation coefficient. The error probability curves are plotted versus the different of the two input SNRs, i.e. $\Delta SNR = SNR_2 - SNR_1(dB)$, with SNR_1 kept constant . Three different crosscorrelation coefficients, $\rho = 0.7$ (corresponding to the high bandwidth efficiency system), $\rho = 0.5$ and $\rho = 1/3$ are considered. The constraints mentioned above are applied to avoid the possible cancelation of the stronger signal at its output side. To assure the accuracy of the Monte-Carlo method, the error probability is estimated after at least 10 bits in error are observed. The error probability curves for three different ρ's are depicted in Figures 4.5, 4.6 and 4.7. Observing the curves from the simulation and the computation in the Section 4.1.2, we can see that they match very well.

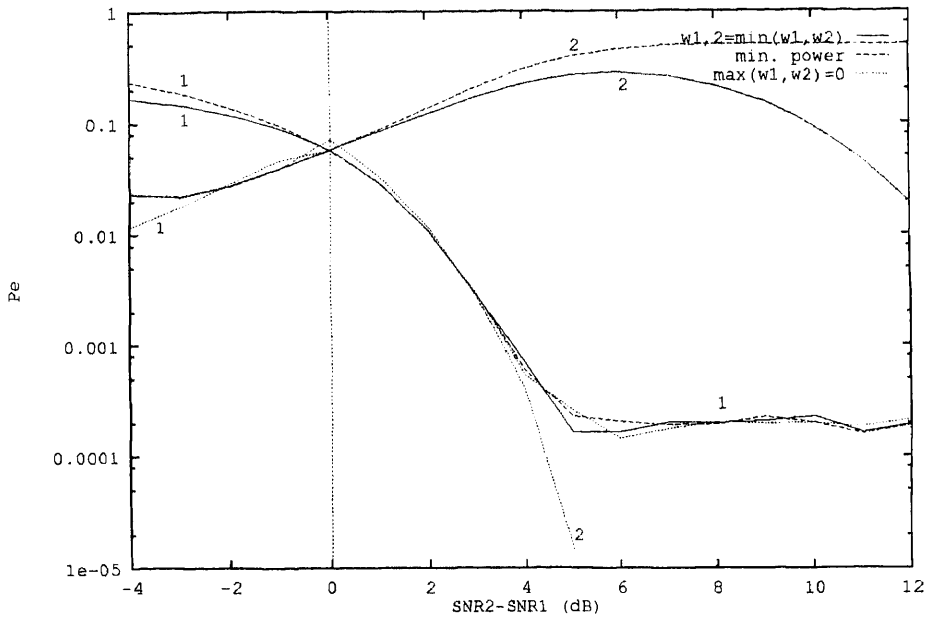

Figure 4.5 Simulated error performance with bit estimates obtained from conventional detector with $\rho = 0.7$, and $SNR_1 = 8$ dB.

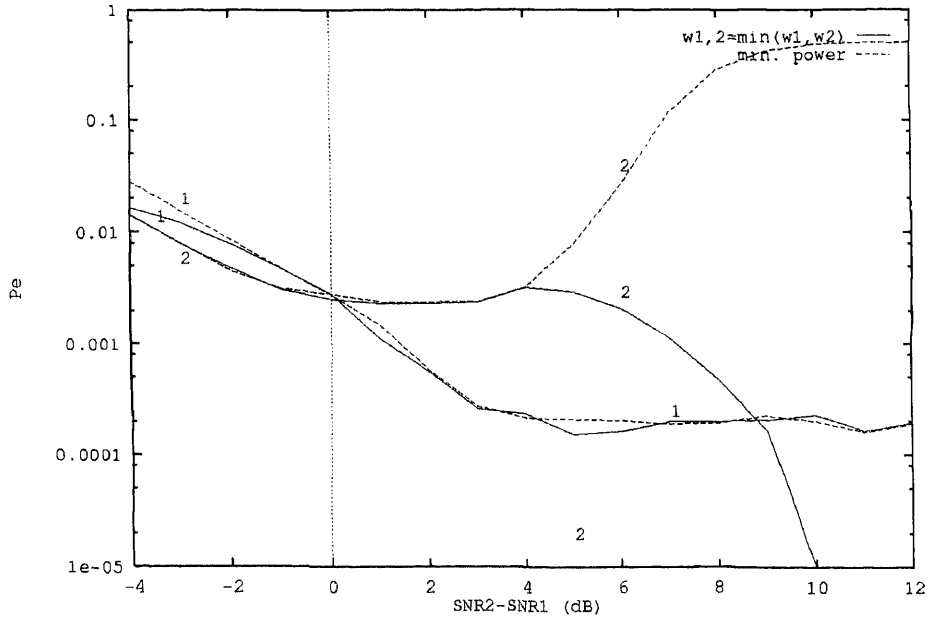

Figure 4.6 Simulated error performance with bit estimates obtained from conventional detector with $\rho = 0.5$, and $SNR_1 = 8$ dB.

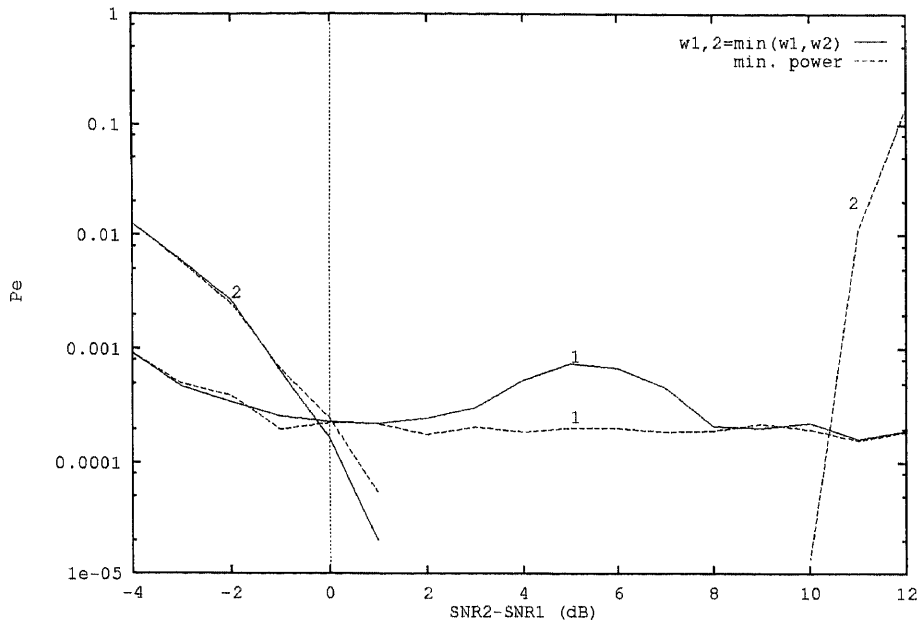

Figure 4.7 Simulated error performance with bit estimates obtained from conventional detector with $\rho = 1/3$, and $SNR_1 = 8$ dB.

2. Convergence speed

In the adaptive canceler, the speed of convergence is also interesting. With the minimum power method, weights are updated at each iteration and will reach their optimum values if the iteration converges. The stability and the speed of convergence is determined by μ in (4.1). A simulation has been done to observe the performance of the weights as μ varies for different input signal-to-noise ratios. Figure 4.8 and Figure 4.9 are the curves for w_1 and w_2 versus the iteration step, where $SNR_1 = SNR_2 = 8dB$, $\rho = 0.7$. Figure 4.10 and Figure 4.11 are those for $SNR_1 = 8dB$, $SNR_2 = 14dB$ and $\rho = 0.7$. μ varies from 0.0002 to 0.002 in both cases.

From the curves shown above we can see that, when $\mu = 0.0002$, convergence occurs at around 20,000 bits, while it is achieved at about 2,000 bits when $\mu = 0.002$. The larger the μ is, the faster the convergence is approached. Of course μ cannot exceed its limitation, otherwise the weights will diverge and the system performance collapses. It also can be seen that the fluctuation of the weights occurs for the case of large value of μ, while convergence gets fast. The performance on $\mu = 0.0008$ gives fast convergence and little fluctuation.

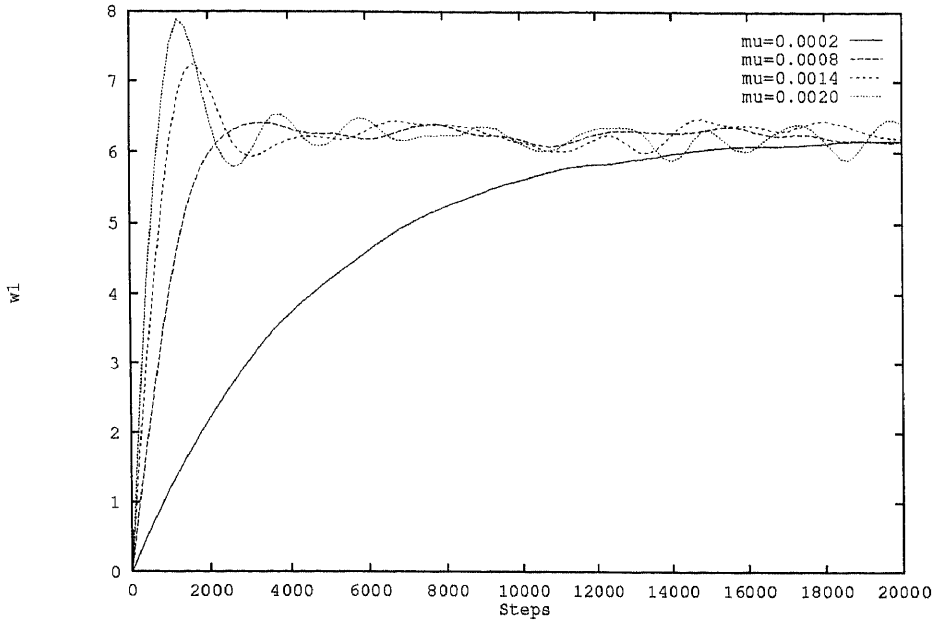

Figure 4.8 Weight (w_1) convergence-bit estimates obtained from conventional detector. $\rho = 0.7$, $SNR_1 = SNR_2 = 8dB$

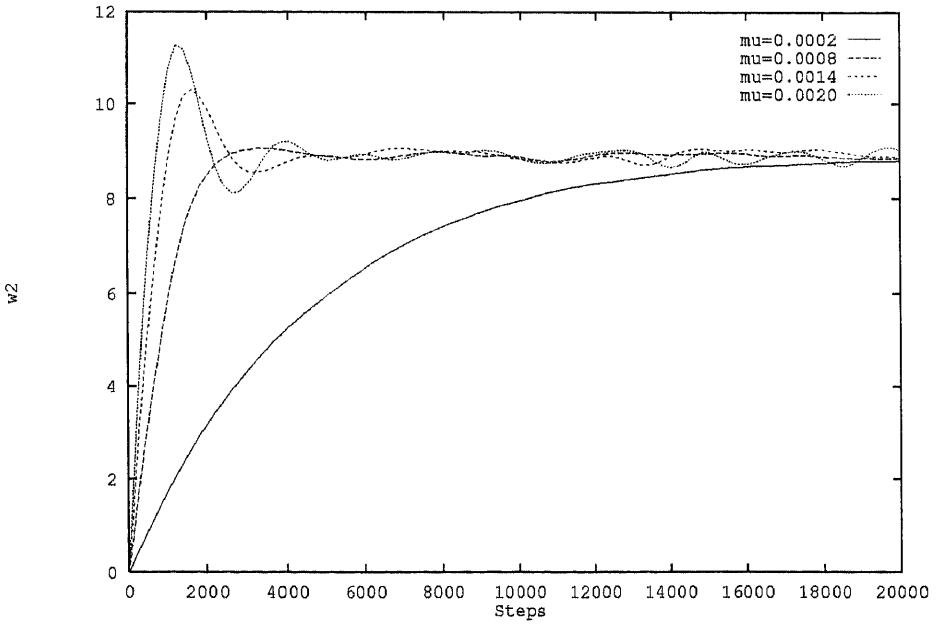

Figure 4.9 Weight (w_2) convergence-bit estimates obtained from conventional detector. $\rho = 0.7$, $SNR_1 = SNR_2 = 8dB$

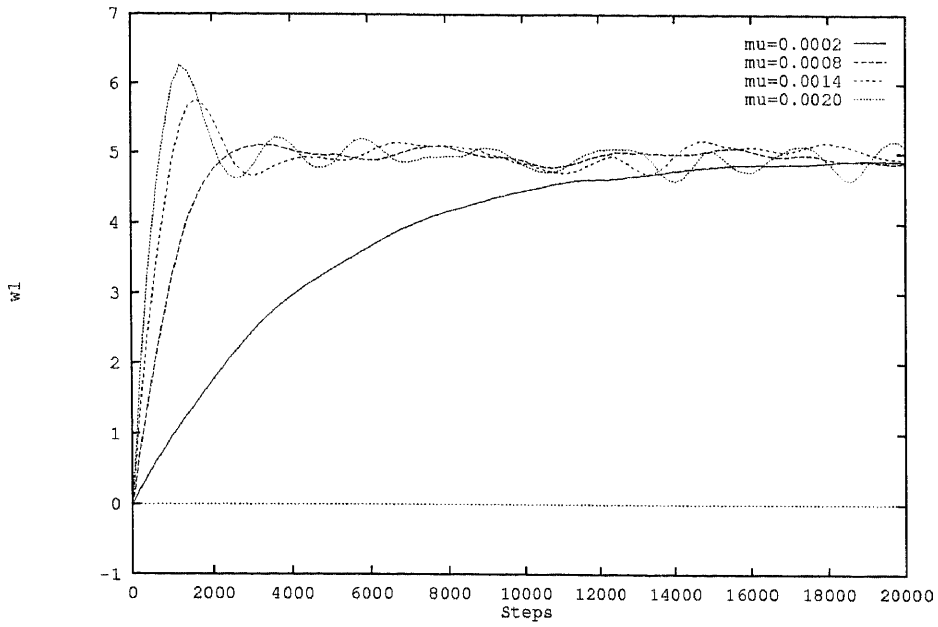

Figure 4.10 Weight (w_1) convergence–bit estimates obtained from conventional detector. $\rho = 0.7$, $SNR_1 = 8$ dB and $SNR_2 = 14dB$

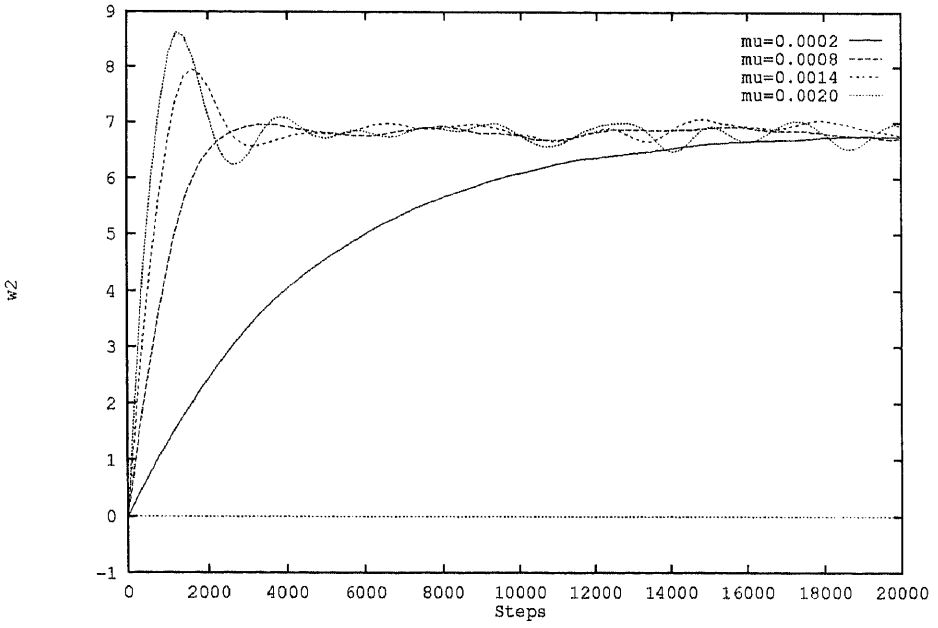

Figure 4.11 Weight (w_2) convergence–bit estimates obtained from conventional detector. $\rho = 0.7$, $SNR_1 = 8$ dB and $SNR_2 = 14dB$

4.2 Adaptive Scheme with Bit Estimates Obtained from Decorrelator Outputs

4.2.1 Scheme

Another structure of the CDMA detector is shown in Figure 4.12. The decision system consists of two stages. The first one is a decorrelating detector that provides the initial bit estimates, followed by adaptive interference canceler.

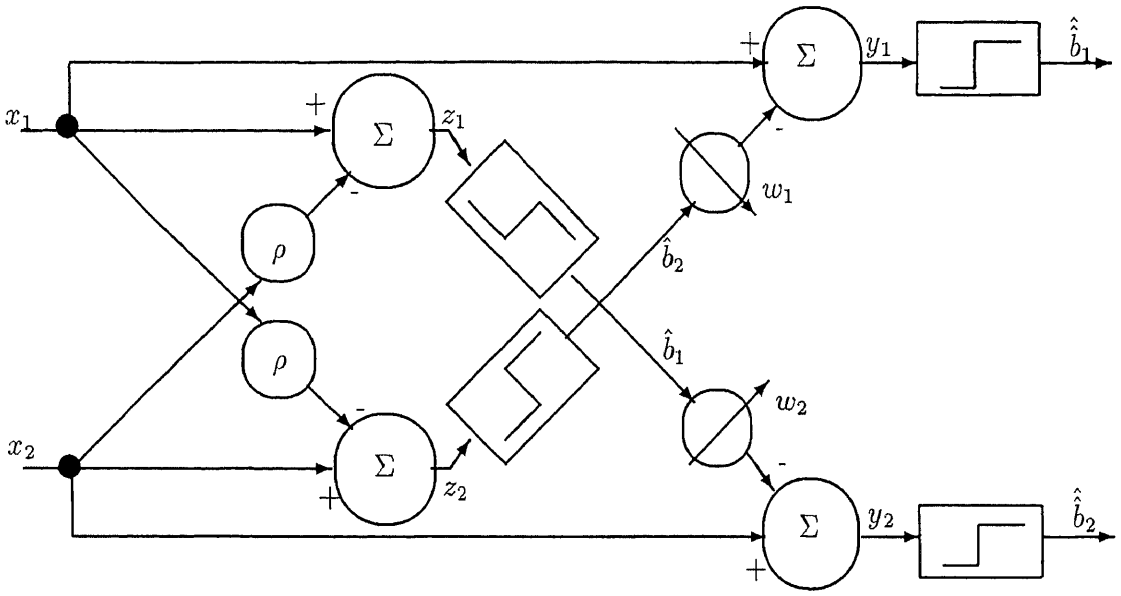

Figure 4.12 Two-stage receiver for two synchronous users–bit estimates obtained by decorrelator

The weights are updated iteratively by the control algorithm that simultaneously minimizes the output powers $E\{y_1^2\}$ and $E\{y_2^2\}$. The optimum weights are obtained the same way as in (4.1)

$$w_j(n+1) = w_j(n) - \mu \frac{dE\{y_j^2(n)\}}{dw_j}, j = 1, 2$$

The outputs of the canceler are as in (4.6) and (4.7). Applying the same derivation shown in (4.2) through (4.5), and considering (2.21) through (2.24), we get

$$\begin{aligned} w_{10} &= \sqrt{A_1}E\{b_2\hat{b}_2\} + \rho\sqrt{A_2}E\{b_1\hat{b}_2\} + E\{n_1\hat{b}_2\} \\ &= \rho\sqrt{A_2}E\{b_2\hat{b}_2\} \end{aligned} \tag{4.22}$$

$$\begin{aligned} w_{20} &= \sqrt{A_2}E\{b_1\hat{b_1}\} + \rho\sqrt{A_1}E\{b_2\hat{b_1}\} + E\{n_2\hat{b_1}\} \\ &= \rho\sqrt{A_1}E\{b_1\hat{b_1}\} \end{aligned} \tag{4.23}$$

By the substitution of (4.22) and (4.23) into (4.6) and (4.7), it is shown that the canceler outputs become

$$y_{10} = \sqrt{A_1}b_1 + \rho\sqrt{A_2}[b_2 - E\{b_2\hat{b_2}\}\hat{b_2}] + n_1 \tag{4.24}$$

$$y_{20} = \sqrt{A_2}b_2 + \rho\sqrt{A_1}[b_1 - E\{b_1\hat{b_1}\}\hat{b_1}] + n_2 \tag{4.25}$$

in which

$$\begin{aligned} E\{b_2\hat{b_2}\} &= Pr(b_2 = \hat{b_2}) - Pr(b_2 \neq \hat{b_2}) \\ &= 1 - 2Pi_2(\epsilon) \end{aligned}$$

But

$$\begin{aligned} Pi_2(\epsilon) &= Pr(\hat{b_2} = 1|b_2 = -1)Pr(b_2 = -1) + Pr(\hat{b_2} = -1|b_2 = 1)Pr(b_2 = 1) \\ &= \frac{1}{2}Pr\left\{\eta_1 > (1-\rho^2)\sqrt{A_2}\right\} + \frac{1}{2}Pr\left\{\eta_1 < -(1-\rho^2)\sqrt{A_2}\right\} \\ &= \frac{1}{2}Q\left(\frac{(1-\rho^2)\sqrt{A_2}}{\sqrt{(1-\rho^2)N_0/2}}\right) + \frac{1}{2}\left[1 - Q\left(\frac{-(1-\rho^2)\sqrt{A_2}}{\sqrt{(1-\rho^2)N_0/2}}\right)\right] \\ &= Q\left(\sqrt{\frac{(1-\rho^2)A_2}{N_0/2}}\right) \end{aligned} \tag{4.26}$$

hence

$$E\{b_2\hat{b_2}\} = 1 - 2Q\left(\sqrt{\frac{(1-\rho^2)A_2}{N_0/2}}\right) \tag{4.27}$$

Similarly

$$E\{b_1\hat{b_1}\} = 1 - 2Q\left(\sqrt{\frac{(1-\rho^2)A_1}{N_0/2}}\right) \tag{4.28}$$

From (4.24) and (4.25) it can be seen that, if the bit estimates of the decorrelator's outputs are almost perfect, i.e. $\hat{b}_1 \simeq b_1$ and $\hat{b}_2 \simeq b_2$, the decision at the canceler output becomes interference free, i.e.

$$y_1 \simeq \sqrt{A_1}b_1 + n_1$$

and

$$y_2 \simeq \sqrt{A_2} b_2 + n_2$$

The error probability of the detection is then determined by the input signal-to-noise ratios $SNR_1 = A_1/N_0$ and $SNR_2 = A_2/N_0$.

The two schemes depicted in Figure 2.5 and Figure 4.12 are identical in the aspects that in both case the input signals are decorrelated and then used as the references to an interference canceler. The only difference between them is that the adaptive weight adjustment is employed in the latter, while the weights are fixed in the former with the knowledge of the received energies. The outputs of interference canceler are the estimates of the signals, which are shown as (2.25), (2.26) and (4.24), (4.25). Assume the input signal-to-noise ratio of user 1, SNR_1 is same for the both case, and that of user 2, SNR_2 is very small so that $\hat{b}_2$ can not make correct estimate at a high probability, hence, error is likely to happen. From (2.25), when $\hat{b}_2$ is a wrong estimate, i.e. $\hat{b}_2 \neq b_2$, since $b_2, \hat{b}_2 \in \{1, -1\}$, the residual interference term becomes

$$\rho\sqrt{A_2}(b_2 - \hat{b}_2) = \pm 2\rho\sqrt{A_2} \tag{4.29}$$

which results in interference doubling. At the same time, the residual interference in (4.24) remains

$$\rho\sqrt{A_2}[b_2 - E\{b_2\hat{b}_2\}\hat{b}_2] \tag{4.30}$$

in which $\left|E\{b_2\hat{b}_2\}\right| \leq 1$. It is easy to see that

$$\left|\rho\sqrt{A_2}[b_2 - E\{b_2\hat{b}_2\}\hat{b}_2]\right| \leq \left|2\rho\sqrt{A_2}\right|$$

i.e. the interference increasing in (4.24) will not be greater than the interference doubling in (2.25). Therefore, from the view of statistics, the scheme of adaptive weights will not be worse than that of fixed weights, even better in low input signal-to-noise ratio situation. Same conclusion can be drawn when SNR_1 is low.

4.2.2 Error Performance

For the detector proposed in Section 4.2.1, the error probability for user 1 is

$$\begin{aligned}
Po_1(\epsilon) &= E_{b_1,b_2,\hat{b_2}} Pr\{\hat{\hat{b}_1} \text{ in error} | b_1, b_2, \hat{b}_2\} \\
&= \frac{1}{2} \sum_{b_2,\hat{b_2}} \Big[Pr(n_1 > \sqrt{A_1} - \rho\sqrt{A_2} b_2 + w_{10}\hat{b_2}) Pr(\hat{b_2}|b_2) Pr(b_2) \\
&\qquad + Pr(n_1 < -\sqrt{A_1} - \rho\sqrt{A_2} b_2 + w_{10}\hat{b_2}) Pr(\hat{b_2}|b_2) Pr(b_2) \Big] \\
&= \frac{1}{4} \sum_{\hat{b_2}} \Bigg\{ \Bigg[Q\left(\frac{\sqrt{A_1} + \rho\sqrt{A_2} + w_{10}\hat{b_2}}{\sqrt{N_0/2}} \right) \\
&\qquad + Q\left(\frac{\sqrt{A_1} - \rho\sqrt{A_2} - w_{10}\hat{b_2}}{\sqrt{N_0/2}} \right) \Bigg] Pr(\hat{b_2}|b_2 = -1) \\
&\qquad + \Bigg[Q\left(\frac{\sqrt{A_1} - \rho\sqrt{A_2} + w_{10}\hat{b_2}}{\sqrt{N_0/2}} \right) \\
&\qquad + Q\left(\frac{\sqrt{A_1} + \rho\sqrt{A_2} - w_{10}\hat{b_2}}{\sqrt{N_0/2}} \right) \Bigg] Pr(\hat{b_2}|b_2 = 1) \Bigg\}
\end{aligned} \tag{4.31}$$

Since, for example

$$\begin{aligned}
Pr(\hat{b_2} = 1 | b_2 = -1) &= Pr\left\{ \eta_2 > (1-\rho^2)\sqrt{A_2} \right\} \\
&= Q\left(\sqrt{\frac{(1-\rho^2)A_2}{N_0/2}} \right)
\end{aligned} \tag{4.32}$$

after averaging over $\hat{b_2}$

$$\begin{aligned}
Po_1(\epsilon) &= \frac{1}{2} \Bigg\{ \Bigg[Q\left(\frac{\sqrt{A_1} + \rho\sqrt{A_2} - w_{10}}{\sqrt{N_0/2}} \right) + Q\left(\frac{\sqrt{A_1} - \rho\sqrt{A_2} + w_{10}}{\sqrt{N_0/2}} \right) \Bigg] \\
&\qquad \cdot \left[1 - Q\left(\sqrt{\frac{(1-\rho^2)A_2}{N_0/2}} \right) \right] \\
&\qquad + \Bigg[Q\left(\frac{\sqrt{A_1} - \rho\sqrt{A_2} - w_{10}}{\sqrt{N_0/2}} \right) + Q\left(\frac{\sqrt{A_1} + \rho\sqrt{A_2} + w_{10}}{\sqrt{N_0/2}} \right) \Bigg] \\
&\qquad \cdot Q\left(\sqrt{\frac{(1-\rho^2)A_2}{N_0/2}} \right) \Bigg\}
\end{aligned} \tag{4.33}$$

Similarly,

$$
\begin{aligned}
Po_2(\epsilon) \;=\; & \frac{1}{2}\left\{\left[Q\left(\frac{\sqrt{A_2}+\rho\sqrt{A_1}-w_{20}}{\sqrt{N_0/2}}\right)+Q\left(\frac{\sqrt{A_2}-\rho\sqrt{A_1}+w_{20}}{\sqrt{N_0/2}}\right)\right]\right. \\
& \cdot\left[1-Q\left(\sqrt{\frac{(1-\rho^2)A_1}{N_0/2}}\right)\right] \\
& +\left[Q\left(\frac{\sqrt{A_2}-\rho\sqrt{A_1}-w_{20}}{\sqrt{N_0/2}}\right)+Q\left(\frac{\sqrt{A_2}+\rho\sqrt{A_1}+w_{20}}{\sqrt{N_0/2}}\right)\right] \\
& \left.\cdot Q\left(\sqrt{\frac{(1-\rho^2)A_1}{N_0/2}}\right)\right\} \qquad (4.34)
\end{aligned}
$$

where w_{10} and w_{20} are, as (4.22) and (4.23)

$$w_{10} = \rho\sqrt{A_2}E\{b_2\hat{b}_2\}$$

$$w_{20} = \rho\sqrt{A_1}E\{b_1\hat{b}_1\}$$

$E\{b_1\hat{b}_1\}$ and $E\{b_2\hat{b}_2\}$ are as (4.28) and (4.27).

Numerical results from the computation of the error probability are presented as the functions of signal-to-noise ratio and the crosscorrelation coefficients. For comparison, the error curves for the canceler with fixed weights in [3] are also plotted. All the error curves are plotted versus ΔSNRs (ranging from -10dB to 12dB), with SNR_1 kept constant.

Same crosscorrelation values as before, ρ = 0.7, 0.5 and 1/3 are used in Figures 4.13, 4.14, 4.15 respectively. Signal from user 1 is considered as desired signal while that from user 2, interference. The performance of user 2 improves as ΔSNR increases. Now we consider the performance of user 1.

Instead of coming from the conventional detector in Section 4.1, the bit estimates here come from the decorrelator whose performance is invariant to the interfering signal energies. From the figures it is seen that the error probability of the decorrelator remains unchanged with interfering signal strength. Due to its error performance invariance to the received signals' energies, the decorrelator is an excellent

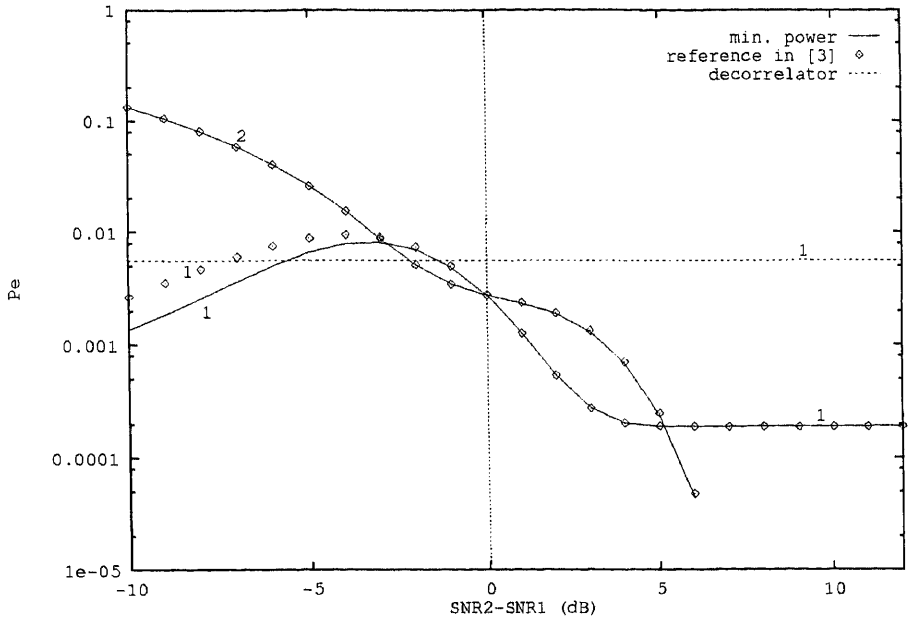

Figure 4.13 Computed error performance with bit estimates obtained from decorrelator with $\rho = 0.7$, and $SNR_1 = 8$ dB.

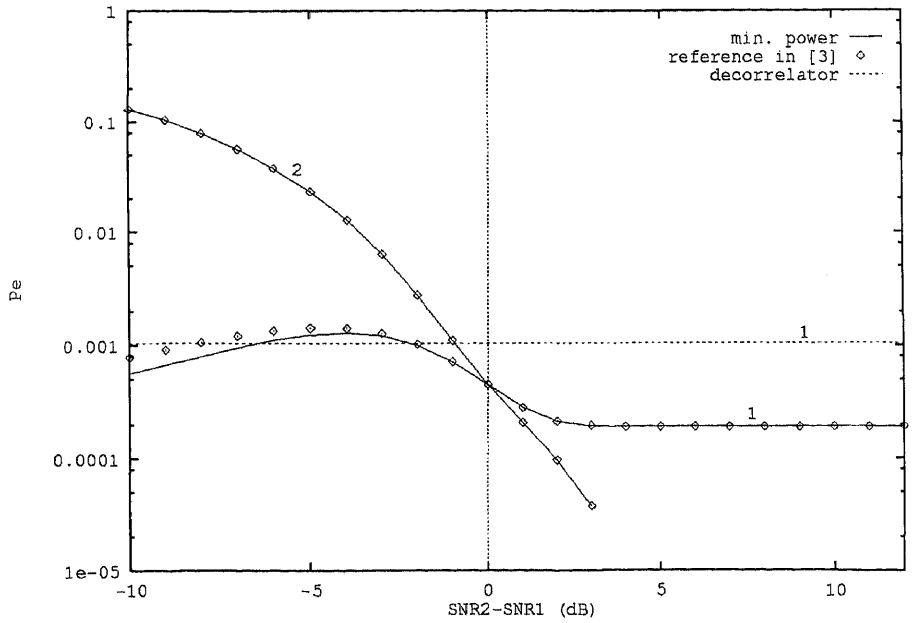

Figure 4.14 Computed error performance with bit estimates obtained from decor relator with $\rho = 0.5$, and $SNR_1 = 8$ dB.

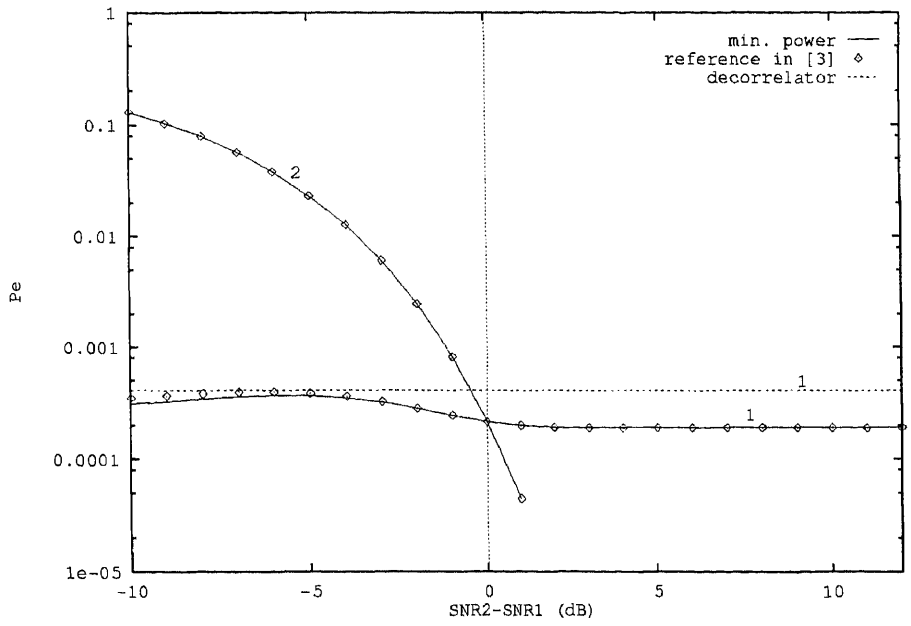

Figure 4.15 Computed error performance with bit estimates obtained from decorrelator with $\rho = 1/3$, and $SNR_1 = 8$ dB.

choice for the first stage. It is also noticed that the considerable performance degradation of the decorrelator occurs with the increasing value of ρ. The degradation results from the decrease of the signal-to-noise ratio at the output of the decorrelator in comparison to its input, as shown in (2.27).

The performance of user 1 improves as the interfering user becomes stronger. When the interfering signal is sufficiently strong, it is the noise, rather than interference that is a primary source of errors, since the interfering signal is estimated very well and hence it is completely canceled. Thus, the error probabilities of user 1 in the figures remain constant when the energy of user 2 keeps increasing, in which case the interference is totally canceled so that only SNR_1 determine the error performance.

When the interfering signal is weaker, it is observed that the error probabilities of two-stage detectors are only marginally higher than those of the decorrelator for some range of ΔSNR. The explanation of the behavior is straightforward. The interfering signal's bits are not well estimated and therefore the cancelation is not always

successful. The adaptive canceler adaptively displays better performance than one with fixed weights as in [3], when the interfering signal energy is lower as predicted in Section 4.2.1. On the other hand, in the high interfering signal energy situation, the performance of the both schemes becomes identical.

4.2.3 Simulation

1. Simulation on error performance

A simulation is conducted with $\rho = 0.7$, 0.5 and 1/3 respectively. SNR_1 is fixed at 8 dB, while $\Delta SNR = SNR_2 - SNR_1$ (dB) varies from -4 dB to 12 dB. The output error probability is plotted with respect to ΔSNR and the crosscorrelation coefficients. Observing Figures 4.16, 4.17, 4.18 we notice that they match Figures 4.13, 4.14, 4.15 respectively.

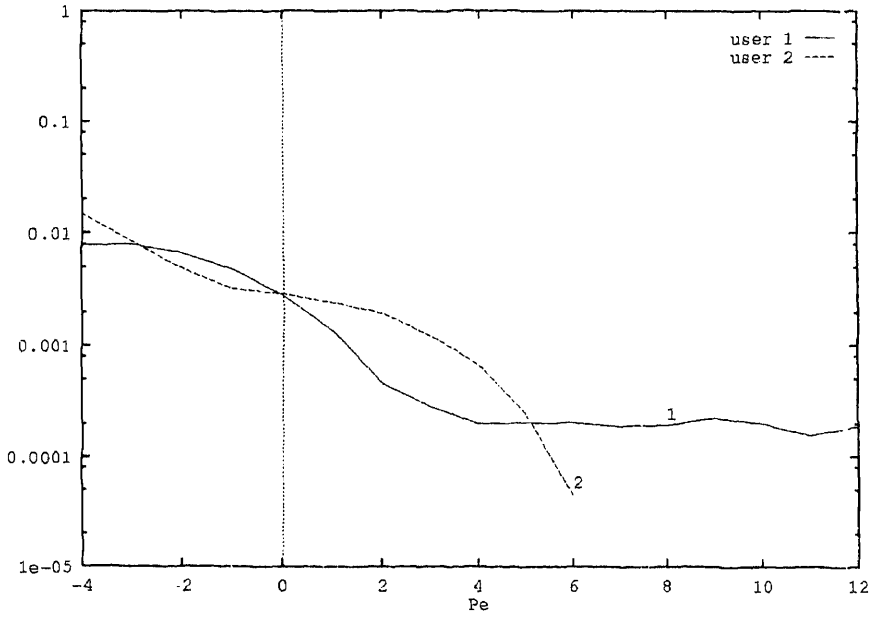

Figure 4.16 Simulated error performance with bit estimates obtained from decorrelat or with $\rho = 0.7$, and $SNR_1 = 8$ dB.

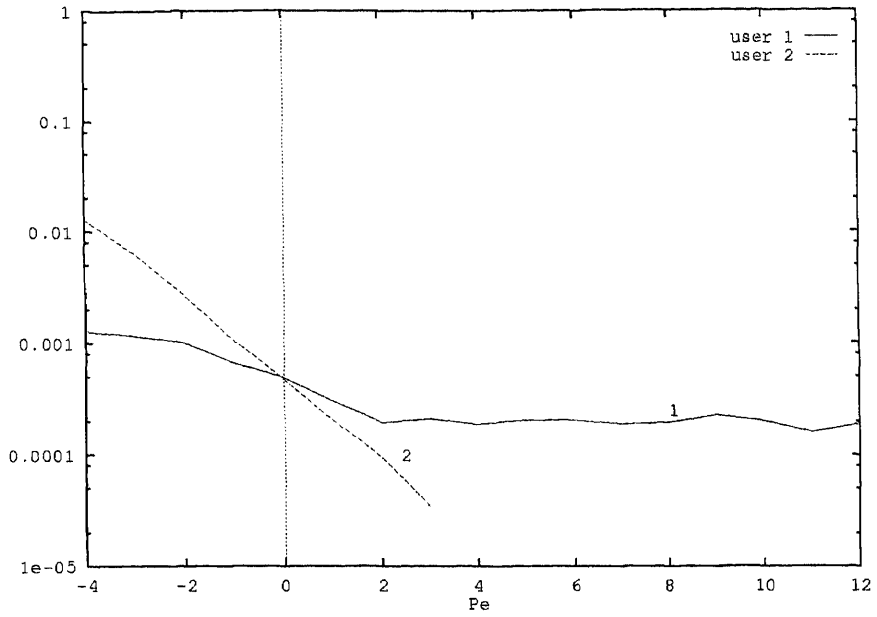

Figure 4.17 Simulated error performance with bit estimates obtained from decorrelat or with $\rho = 0.5$, and $SNR_1 = 8$ dB.

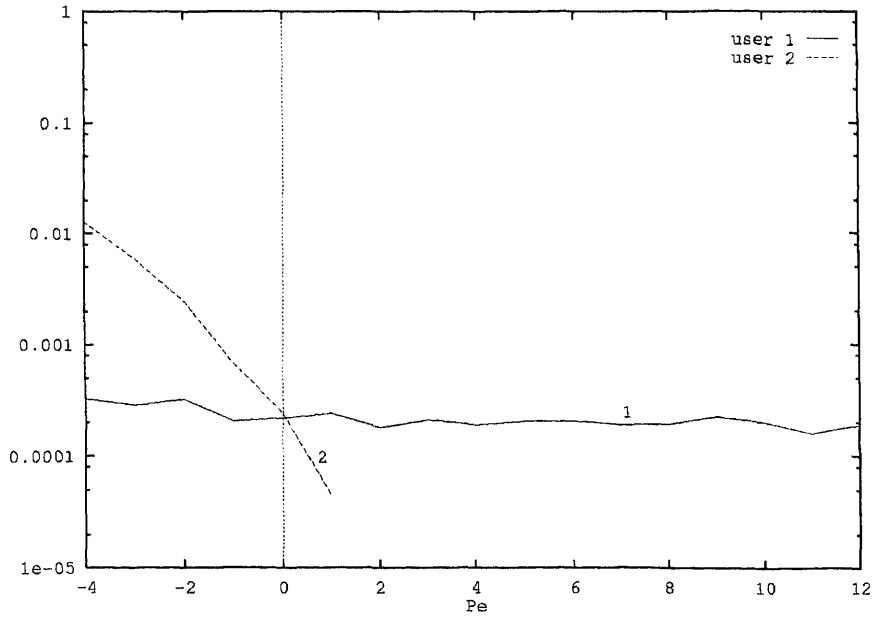

Figure 4.18 Simulated error performance with bit estimates obtained from decorrelat or with $\rho = 1/3$, and $SNR_1 = 8$ dB.

2. Convergence speed

Figures 4.19 to 4.22 are the curves for weights w_1 and w_2. Convergence occurs approximately in 20,000 steps for $\mu = 0.0002$ and much faster for larger μ's. As SNR_1 is fixed at 8 dB, curve of w_2 displays larger fluctuation for $SNR_2 = 14dB$ than that for $SNR_2 = 8dB$. However, the severe fluctuation of w_2 at large SNR_2 is not critical to the error performance. This can be concluded from (4.7)

$$y_2 = \sqrt{A_2}b_2 + \rho\sqrt{A_1}b_1 - w_2\hat{b}_1 + n_2$$

where the first term of the right-hand side is dominant when much stronger user 2 presents, therefore the correct decision can be achieved even though w_2 fluctuates heavily.

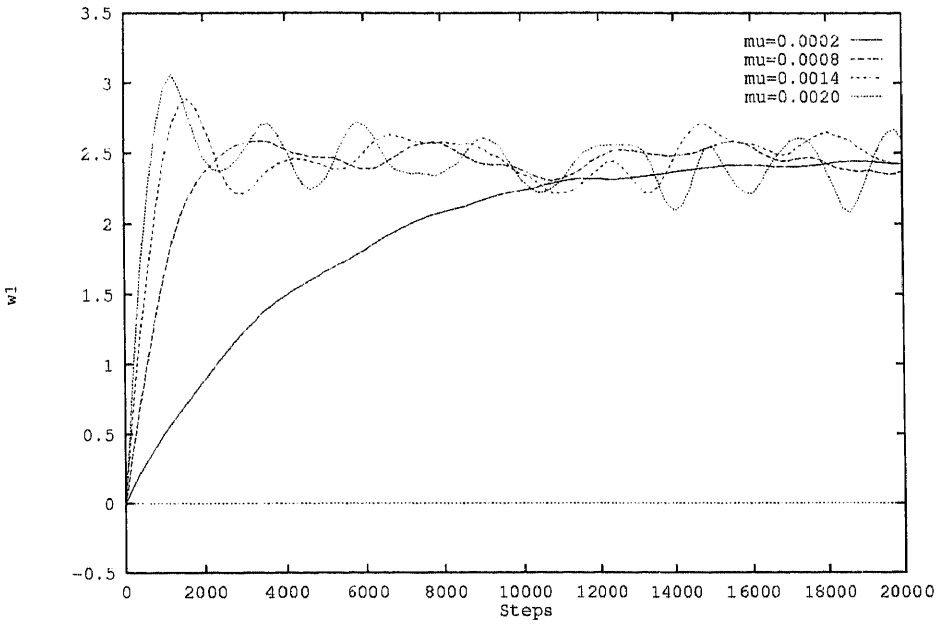

Figure 4.19 Weight (w_1) convergence–bit estimates obtained from decorrelator. $\rho = 0.7$, $SNR_1 = SNR_2 = 8dB$

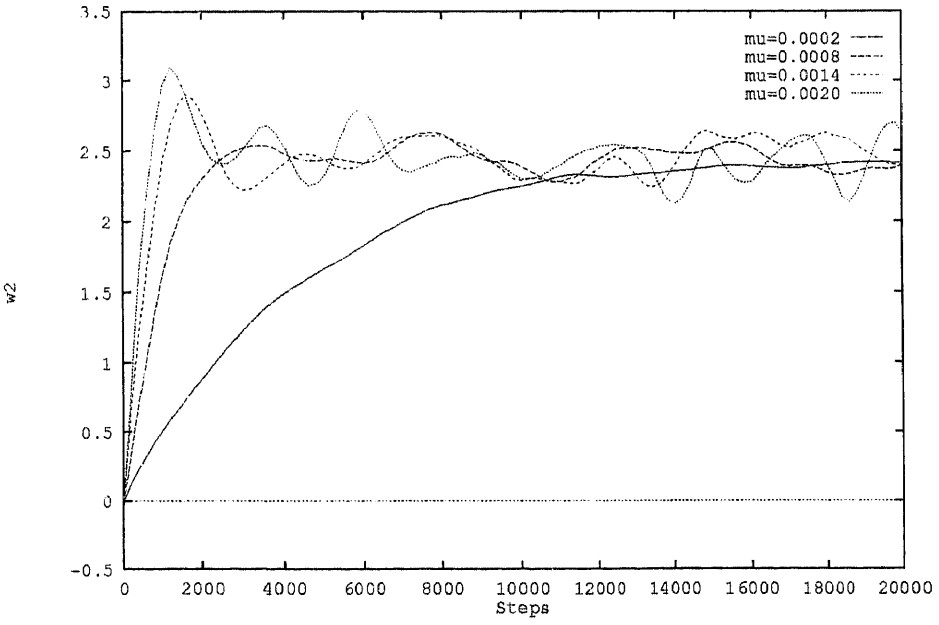

Figure 4.20 Weight (w_2) convergence–bit estimates obtained from decorrelator. $\rho = 0.7$, $SNR_1 = SNR_2 = 8dB$

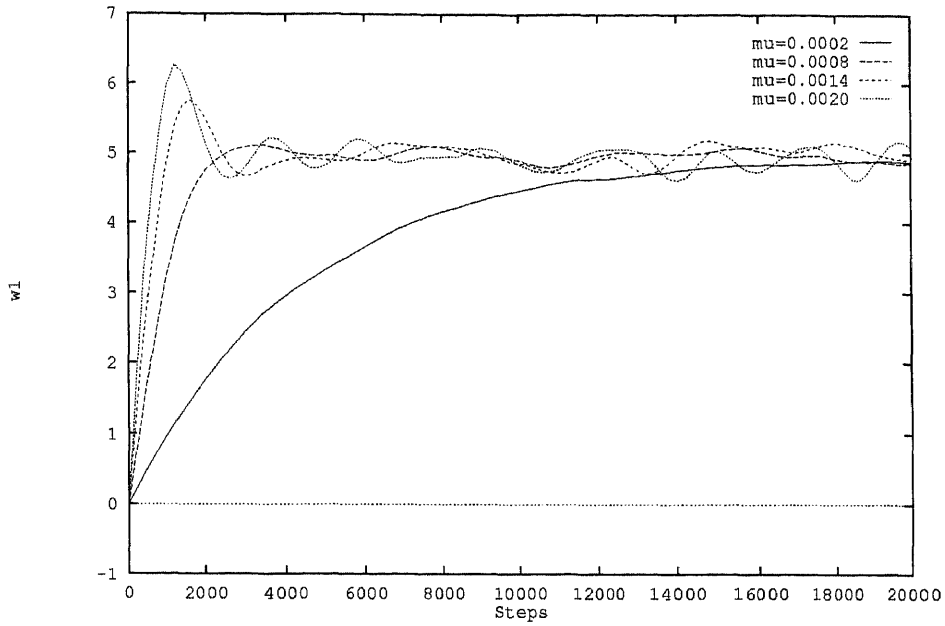

Figure 4.21 Weight (w_1) convergence–bit estimates obtained from decorrelator. $\rho = 0.7$, $SNR_1 = 8$ dB and $SNR_2 = 14dB$

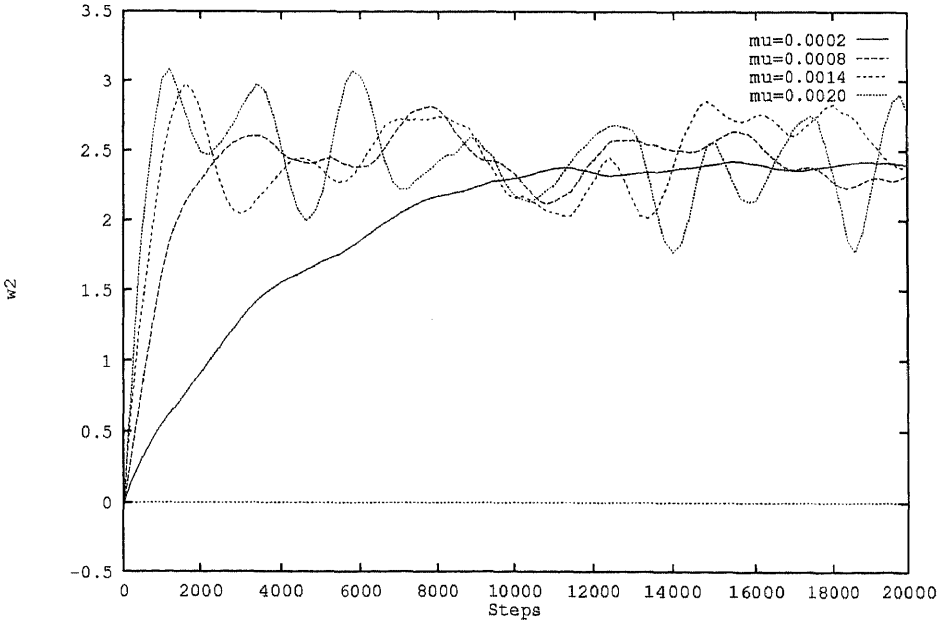

Figure 4.22 Weight (w_2) convergence–bit estimates obtained from decorrelator. $\rho = 0.7$, $SNR_1 = 8$ dB and $SNR_2 = 14dB$

CHAPTER 5

CONCLUSIONS

A synchronous two-stage CDMA detector for two users which did not require knowledge of energies of received signals, was discussed and analyzed. For the decision system employing adaptive canceler based on the bit estimate coming from conventional single user detector, constraint strategies were imposed to successfully prevent the performance degradation of the stronger user due to the power inversion effect. The two-stage detector based on the decorrelating first stage was shown to perform significantly better than the conventional detector, decorrelating detector and the two-stage detectors based on conventional detecting first stage. With the strong interference present, its performance approaches the performance of an optimum detector. In the presence of weak interfering signal, the adaptive scheme displayed better performance than the fixed-weight scheme. Furthermore, the adaptive scheme did not require the knowledge of the received signal energies while fixed-weight scheme did. Therefore, there is no need for estimation of the received signal energies.

In the adaptive canceler, weights were adjusted in each iteration, and converged to their optimum values. The iterative stability and convergence speed were determined by the factor μ. Large fluctuation of weight performance occurred when one user was much stronger than the other. However, the system performance was hardly affected by the fluctuation due to the dominant strength of the stronger user.

The future work should include the multi user detector (user number is greater than two), different adaptive weight control algorithms and asyschronous signal environment.

REFERENCES

1. S. Verdu, "Recent Progress in Multiuser Detection," *Advances in Communications and Signal Processing*, W.A. Poter and S.C. Kak Ed., Springer-Verlag, 1988.

2. Y. Bar-Ness, A. Dinc and H. Messer, "Bootstrapped Adaptive Separation of Superimposed Signals - Analysis of the Effect of Thermal Noise on Performance," submitted for publication, 1993.

3. M. Varanasi and B. Aazhang, "Near-Optimum Detection in Synchronous Code-Division Multiple-Access Systems," *IEEE Trans. Commun.*, Vol. 39, No. 5, May 1991.

4. Z. Siveski and Y. Bar-Ness, "Adaptive Two-Stage Detection Scheme in Synchronous Two-User CDMA Systems," submitted for presentation at Milcom, 1993.

5. Z. Siveski, Y. Bar-Ness, and W.P. Chen, "Adaptive Detection Scheme for Synchronous CDMA Systems," in final preparation, 1993.